What Do We Understand About Convolutional Networks?

Isma Hadji and Richard P. Wildes

Department of Electrical Engineering and Computer Science

York University

Toronto, Ontario

Canada

Chapter 1

Introduction

1.1 Motivation

Over the past few years major computer vision research efforts have focused on convolutional neural networks, commonly referred to as ConvNets or CNNs. These efforts have resulted in new state-of-the-art performance on a wide range of classification (e.g [64, 88, 139]) and regression (e.g [36, 97, 159]) tasks. In contrast, while the history of such approaches can be traced back a number of years (e.g [49, 91]), theoretical understanding of how these systems achieve their outstanding results lags. In fact, currently many contributions in the computer vision field use ConvNets as a black box that works while having a very vague idea for why it works, which is very unsatisfactory from a scientific point of view. In particular, there are two main complementary concerns: **(1)** For learned aspects (e.g convolutional kernels), exactly what has been learned? **(2)** For architecture design aspects (e.g number of layers, number of kernels/layer, pooling strategy, choice of nonlinearity), why are some choices better than others? The answers to these questions not only will improve the scientific understanding of ConvNets, but also increase their practical applicability.

Moreover, current realizations of ConvNets require massive amounts of data for training [84, 88, 91] and design decisions made greatly impact performance [23, 77]. Deeper theoretical understanding should lessen dependence on data-driven design. While empirical studies have investigated the operation of implemented networks, to

date, their results largely have been limited to visualizations of internal processing to understand what is happening at the different layers of a ConvNet [104, 133, 154].

1.2 Objective

In response to the above noted state of affairs, this document will review the most prominent proposals using multilayer convolutional architectures. Importantly, the various components of a typical convolutional network will be discussed through a review of different approaches that base their design decisions on biological findings and/or sound theoretical bases. In addition, the different attempts at understanding ConvNets via visualizations and empirical studies will be reviewed. The ultimate goal is to shed light on the role of each layer of processing involved in a ConvNet architecture, distill what we currently understand about ConvNets and highlight critical open problems.

1.3 Outline of report

This report is structured as follows: The present chapter has motivated the need for a review of our understanding of convolutional networks. Chapter 2 will describe various multilayer networks and present the most successful architectures used in computer vision applications. Chapter 3 will more specifically focus on each one of the building blocks of typical convolutional networks and discuss the design of the different components from both biological and theoretical perspectives. Finally, chapter 4 will describe the current trends in ConvNet design and efforts towards ConvNet understanding and highlight some critical outstanding shortcomings that remain.

Chapter 2

Multilayer Networks

This chapter gives a succinct overview of the most prominent multilayer architectures used in computer vision, in general. Notably, while this chapter covers the most important contributions in the literature, it will not to provide a comprehensive review of such architectures, as such reviews are available elsewhere (*e.g.* [17, 56, 90]). Instead, the purpose of this chapter is to set the stage for the remainder of the document and its detailed presentation and discussion of what currently is understood about convolutional networks applied to visual information processing.

2.1 Multilayer architectures

Prior to the recent success of deep learning-based networks, state-of-the-art computer vision systems for recognition relied on two separate but complementary steps. First, the input data is transformed via a set of hand designed operations (*e.g.* convolutions with a basis set, local or global encoding methods) to a suitable form. The transformations that the input incurs usually entail finding a compact and/or abstract representation of the input data, while injecting several invariances depending on the task at hand. The goal of this transformation is to change the data in a way that makes it more amenable to being readily separated by a classifier. Second, the transformed data is used to train some sort of classifier (*e.g.* Support Vector Machines) to recognize the content of the input signal. The performance of any classifier used is, usually, heavily affected by the used transformations.

Multilayer architectures with learning bring about a different outlook on the problem by proposing to learn, not only the classifier, but also learn the required transformation operations directly from the data. This form of learning is commonly referred to as representation learning [7, 90], which when used in the context of deep multilayer architectures is called deep learning.

Multilayer architectures can be defined as computational models that allow for extracting useful information from the input data multiple levels of abstraction. Generally, multilayer architectures are designed to amplify important aspects of the input at higher layers, while becoming more and more robust to less significant variations. Most multilayer architectures stack simple building block modules with alternating linear and nonlinear functions. Over the years, a plethora of various multilayer architectures were proposed and this section will cover the most prominent such architectures adopted for computer vision applications. In particular, artificial neural network architectures will be the focus due to their prominence. For the sake of succinctness, such networks will be referred to more simply as neural networks in the following.

2.1.1 Neural networks

A typical neural network architecture is made of an input layer, $\boldsymbol{x}$, an output layer, $\boldsymbol{y}$, and a stack of multiple hidden layers, $\boldsymbol{h}$, where each layer consists of multiple cells or units, as depicted in Figure 2.1. Usually, each hidden unit, h_j, receives input from all units at the previous layer and is defined as a weighted combination of the inputs followed by a nonlinearity according to

$$h_j = F(b_j + \sum_i w_{ij} x_i) \tag{2.1}$$

where, w_{ij}, are the weights controlling the strength of the connections between the input units and the hidden unit, b_j is a small bias of the hidden unit and $F(.)$ is some saturating nonlinearity such as the sigmoid.

Deep neural networks can be seen as a modern day instantiation of Rosenblatt's perceptron [122] and multilayer perceptron [123]. Although, neural network models

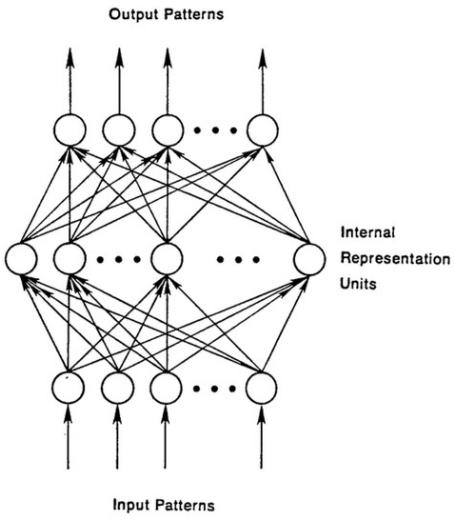

Figure 2.1: Illustration of a typical Neural Network architecture. Figure reproduced from [17].

have been around for many years (*i.e.* since the 1960's) they were not heavily used until more recently. There were a number of reasons for this delay. Initial negative results showing the inability of the perceptron to model simple operations like XOR, hindered further investigation of perceptrons for a while until their generalizations to many layers [106]. Also, lack of an appropriate training algorithm slowed progress until the popularization of the backpropagation algorithm [125]. However, the bigger roadblock that hampered the progress of multilayer neural networks is the fact that they rely on a very large number of parameters, which in turn implies the need for large amounts of training data and computational resources to support learning of the parameters.

A major contribution that allowed for a big leap of progress in the field of deep neural networks is layerwise unsupervised pretraining, using Restricted Boltzman Machine (RBM) [68]. Restricted Boltzman Machines can be seen as two layer neural networks where, in their restricted form, only feedforward connections are allowed. In the context of image recognition, the unsupervised learning method used to train RBMs can be summarized in three steps. First, for each pixel, x_i, and starting with a set of random weights, w_{ij}, and biases, b_j, the hidden state, h_j, of each unit is set to 1 with probability, p_j. The probability is defined as

$$p_j = \sigma(b_j + \sum_i x_i w_{ij}) \tag{2.2}$$

where, $\sigma(y) = 1/(1+exp(-y))$. Second, once all hidden states have been set stochastically based on equation 2.2, an attempt to reconstruct the image is performed by setting each pixel, x_i, to 1 with probability $p_i = \sigma(b_i + \sum_j h_j w_{ij})$. Third, the hidden units are corrected by updating the weights and biases based on the reconstruction error given by

$$\Delta w_{ij} = \alpha(\langle x_i h_j \rangle_{input} - \langle x_i h_j \rangle_{reconstruction}) \tag{2.3}$$

where α is a learning rate and $\langle x_i h_j \rangle$ is the number of times pixel x_i and the hidden unit h_j are on together. The entire process is repeated N times or until the error drops bellow a pre-set threshold, τ. After one layer is trained its outputs are used as an input to the next layer in the hierarchy, which is in turn trained following the same procedure. Usually, after all the network's layers are pretrained, they are further finetuned with labeled data via error back propagation using gradient descent [68]. Using this layerwise unsupervised pretraining allows for training deep neural networks without requiring large amounts of labeled data because unsupervised RBM pretraining provides a way for an empirically useful initialization of the various network parameters.

Neural networks relying on stacked RBMs were first successfully deployed as a method for dimensionality reduction with an application to face recognition [69], where they were used as a type of auto-encoder. Loosely speaking, auto-encoders can be defined as multilayer neural networks that are made of two main parts: First, an encoder transforms the input data to a feature vector; second, a decoder maps the generated feature vector back to the input space; see, Figure 2.2. The parameters of the auto-encoder are learned by minimizing a reconstruction error between the input and it's reconstructed version.

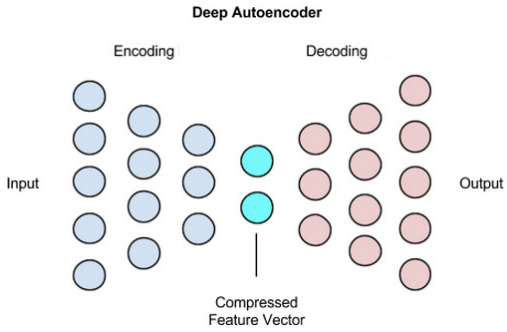

Figure 2.2: Structure of a typical Auto-Encoder Network. Figure reproduced from [17].

Beyond RBM based auto-encoders, several types of auto-encoders were later proposed. Each auto-encoder introduced a different regularization method that prevents the network from learning trivial solutions even while enforcing different invariances. Examples include Sparse Auto-Encoders (SAE) [8], Denoising Auto-Encoders (DAE) [141, 142] and Contractive Auto-Encoders (CAE) [118]. Sparse Auto-Encoders [8] allow the intermediate representation's size (*i.e.* as generated by the encoder part) to be larger than the input's size while enforcing sparsity by penalizing negative outputs. In contrast, Denoising Auto-Encoders [141, 142] alter the objective of the reconstruction itself by trying to reconstruct a clean input from an artificially corrupted version, with the goal being to learn a robust representation. Similarly, Contractive Auto-Encoders [118] build on denoising auto-encoders by further penalizing the units that are most sensitive to the injected noise. More detailed reviews of various types of auto-encoders can be found elsewhere [7].

2.1.2 Recurrent neural networks

When considering tasks that rely on sequential inputs, one of the most successful multilayer architectures is the Recurrent Neural Network (RNN) [9]. RNNs, illustrated in Figure 2.3, can be seen as a special type of neural network where each hidden unit takes input from the the data it observes at the current time step as well as its state at a previous time step. The output of an RNN is defined as

$$h_t = \sigma(w_i x_t + u_i h_{t-1}) \tag{2.4}$$

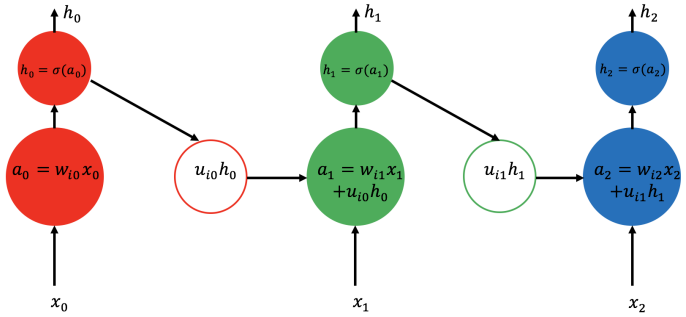

Figure 2.3: Illustration of the operations of a standard Recurrent Neural Network. Each RNN unit takes new input at the current time frame, x_t, and from a previous time step, h_{t-1} and the new output of the unit is calculated according to (2.4) and can be fed to another layer of processing in a multilayer RNN.

where σ is some nonlinear squashing function and w_i and u_i are the network parameters that control the relative importance of the present and past information.

Although RNNs are seemingly powerful architectures, one of their major problems is their limited ability to model long term dependencies. This limitation is attributed to training difficulties due to exploding or vanishing gradient that can occur when propagating the error back through multiple time steps [9]. In particular, during training the back propagated gradient is multiplied with the network's weights from the current time step all the way back to the initial time step. Therefore, because of this multiplicative accumulation, the weights can have a non-trivial effect on the propagated gradient. If weights are small the gradient vanishes, whereas larger weights lead to a gradient that explodes. To correct for this difficulty, Long Short Term Memories (LSTM) were introduced [70].

LSTMs are recurrent networks that are further equipped with a storage or memory component, illustrated in Figure 2.4, that accumulates information over time. An LSTM's memory cell is gated such that it allows information to be read from it or written to it. Notably, LSTMs also contain a forget gate that allows the network to erase information when it is not needed anymore. LSTMs are controlled by three different gates (the input gate, i_t, the forget gate, f_t, and the output gate, o_t), as well as the memory cell state, c_t. The input gate is controlled by the current input, x_t, and the previous state, h_{t-1}, and it is defined as

$$i_t = \sigma(w_i x_t + u_i h_{t-1} + b_i), \tag{2.5}$$

where, w_i, u_i, b_i represent the weights and bias controlling the connections to the input gate and σ is usually a sigmoid function. The forget gate is similarly defined as

$$f_t = \sigma(w_f x_t + u_f h_{t-1} + b_f), \tag{2.6}$$

and it is controlled by its corresponding weights and bias, w_f, u_f, b_f. Arguably, the most important aspect of an LSTM is that it copes with the challenge of vanishing and exploding gradients. This ability is achieved through additive combination of the forget and input gate states in determining the memory cell's state, which, in turn, controls whether information is passed on to another cell via the output gate. Specifically, the cell state is computed in two steps. First, a candidate cell state is estimated according to

$$g_t = \phi(w_c x_t + u_c h_{t-1} + b_c), \tag{2.7}$$

where ϕ is usually a hyperbolic tangent. Second, the final cell state is finally controlled by the current estimated cell state, g_t, and the previous cell state, c_{t-1}, modulated by the input and forget gate according to

$$c_t = i_t g_t + f_t c_{t-1}. \tag{2.8}$$

Finally, using the cell's state and the current and previous inputs, the value of the output gate and the output of the LSTM cell are estimated according to

$$o_t = \sigma(w_o x_t + u_o h_{t-1} + b_o), \tag{2.9}$$

where

$$h_t = \phi(c_t)\, o_t. \tag{2.10}$$

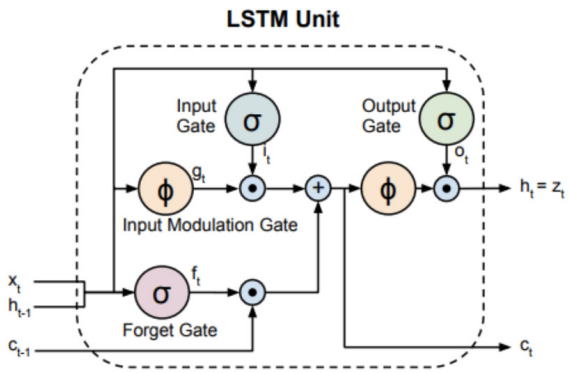

Figure 2.4: Illustration of a typical LSTM unit. The unit takes input at the current time, x_t, and from a previous time, h_{t-1}, and it returns an output to be fed into the next time, h_t. The final output of the LSTM unit is controlled by the input gate, i_t, the forget gate, f_t, and the output gate, o_t, as well as the memory cell state, c_t, which are defined in (2.5), (2.6), (2.9) and (2.8), respectively. Figure reproduced from [33].

2.1.3 Convolutional networks

Convolutional networks (ConvNets) are a special type of neural network that are especially well adapted to computer vision applications because of their ability to hierarchically abstract representations with local operations. There are two key design ideas driving the success of convolutional architectures in computer vision. First, ConvNets take advantage of the 2D structure of images and the fact that pixels within a neighborhood are usually highly correlated. Therefore, ConvNets eschew the use of one-to-one connections between all pixel units (*i.e.* as is the case of most neural networks) in favor of using grouped local connections. Further, ConvNet architectures rely on feature sharing and each channel (or output feature map) is thereby generated from convolution with the same filter at all locations as depicted in Figure 2.5. This important characteristic of ConvNets leads to an architecture that relies on far fewer parameters compared to standard Neural Networks. Second, ConvNets also introduce a pooling step that provides a degree of translation invariance making the architecture less affected by small variations in position. Notably, pooling also allows the network to gradually see larger portions of the input thanks to an increased size of the network's receptive field. The increase in receptive field size (coupled with a decrease in the input's resolution) allows the network to repre-

add more filters, increase receptive field, decrease the input resolution

sent more abstract characteristics of the input as the network's depth increase. For example, for the task of object recognition, it is advocated that ConvNets layers start by focusing on edges to parts of the object to finally cover the entire object at higher layers in the hierarchy.

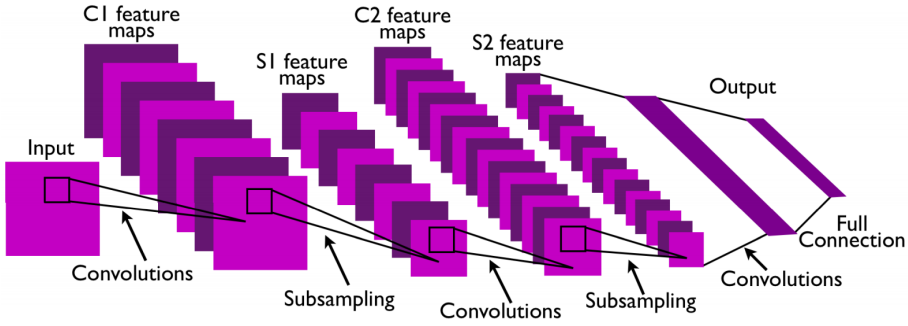

Figure 2.5: Illustration of the structure of a standard Convolutional Network. Figure reproduced from [93].

The architecture of convolutional networks is heavily inspired by the processing that takes place in the visual cortex as described in the seminal work of Hubel and Wiesel [74] (further discussed in Chapter 3). In fact, it appears that the earliest instantiation of Convolutional Networks is Fukushima's Neocognitron [49], which also relied on local connections and in which each feature map responds maximally to only a specific feature type. The Neocognitron is composed of a cascade of K layers where each layer alternates S-cell units, U_{sl}, and complex cell units, U_{cl}, that loosely mimic the processing that takes place in the biological simple and complex cells, respectively, as depicted in Figure 2.6. The simple cell units perform operations similar to local convolutions followed by a Rectified Linear Unit (ReLU) nonlinearity, $\varphi(x) = \begin{cases} x; & if\, x \geq 0 \\ 0; & x < 0 \end{cases}$,while the complex cells perform operations similar to average pooling. The model also included a divisive nonlinearity to accomplish something akin to normalization in contemporary ConvNets.

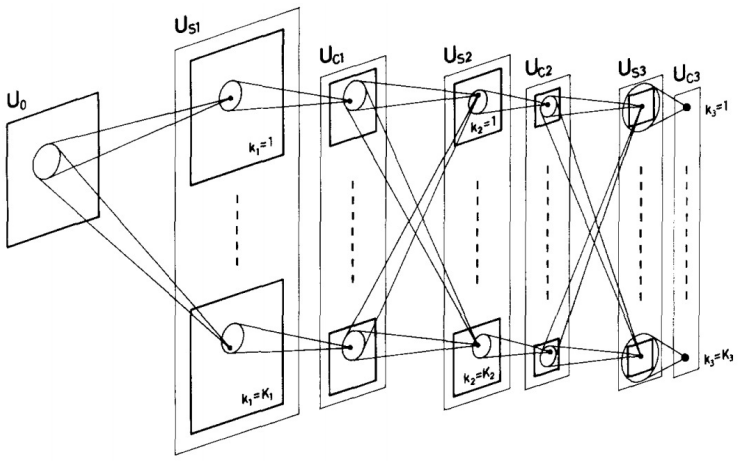

Figure 2.6: Illustration of the structure of the Neocognitron. Figure reproduced from [49].

As opposed to most standard ConvNet architectures (*e.g.* [88,91]) the Neocognitron does not need labeled data for learning as it is designed based on self organizing maps that learn the local connections between consecutive layers via repetitive presentations of a set of stimulus images. In particular, the Neocognitron is trained to learn the connections between an input feature map and a simple cell layer (connections between a simple cells layer and complex cells layer are pre-fixed) and the learning procedure can be broadly summarized in two steps. First, each time a new stimulus is presented at the the input, the simple cells that respond to it maximally are chosen as a representative cell for that stimulus type. Second, the connections between the input and those representative cells are reinforced each time they respond to the same input type. Notably, simple cells layers are organized in different groups or planes such that each plane responds only to one stimulus type (*i.e.* similar to feature maps in a modern ConvNet architecture). Subsequent extensions to the Neocognitron included allowances for supervised learning [51] as well as top-down attentional mechanisms [50].

Most ConvNets architectures deployed in recent computer vision applications are inspired by the successful architecture proposed by LeCun in 1998, now known as LeNet, for handwriting recognition [91]. As described in key literature [77, 93], a classical convolutional network is made of four basic layers of processing: (i) a convolution layer, (ii) a nonlinearity or rectification layer, (iii) a normalization

layer and (iv) a pooling layer. As noted above, these components were largely present in the Neocognitron. A key addition in LeNet was the incorporation of back propagation for relatively efficient learning of the convolutional parameters.

Although, ConvNets allow for an optimized architecture that requires far fewer parameters compared to their fully connected neural network counterpart, their main shortcoming remains their heavy reliance on learning and labeled data. This data dependence is probably one of the main reasons why ConvNets were not widely used until 2012 when the availability of the large ImageNet dataset [126] and concomitant computational resources made it possible to revive interest in ConvNets [88]. The success of ConvNets on ImageNet led to a spurt of various ConvNet architectures and most contributions in this field are merely based on different variations of the basic building blocks of ConvNets, as will be discussed later in Section 2.2.

2.1.4 Generative adversarial networks

Generative Adversarial Networks (GANs) are relatively new models taking advantage of the strong representational power of multilayer architectures. GANs were first introduced in 2014 [57] and although they did not present a different architecture per se (*i.e.* in terms of novel network building blocks for example), they entail some peculiarities, which make them a slightly different class of multilayer architectures. A key challenge being responded to by GANs is the introduction of an unsupervised learning approach that requires no labeled data.

A typical GAN is made of two competing blocks or sub-networks, as shown in Figure 2.7; a generator network, $G(\mathbf{z};\theta_g)$, and a discriminator network, $D(\mathbf{x};\theta_d)$, where $\mathbf{z}$ is input random noise, $\mathbf{x}$ is real input data (*e.g.* an image) and θ_g and θ_d are the parameters of the two blocks, respectively. Each block can be made of any of the previously defined multilayer architectures. In the original paper both the generator and discriminator were multilayer fully connected networks. The discriminator, D, is trained to recognize the data coming from the generator and assigning the label *"fake"* with probability p_d while assigning the label *"real"* to true input data with probability $1 - p_d$. In complement, the generator network is optimized to generate fake representations capable of fooling the discriminator. The

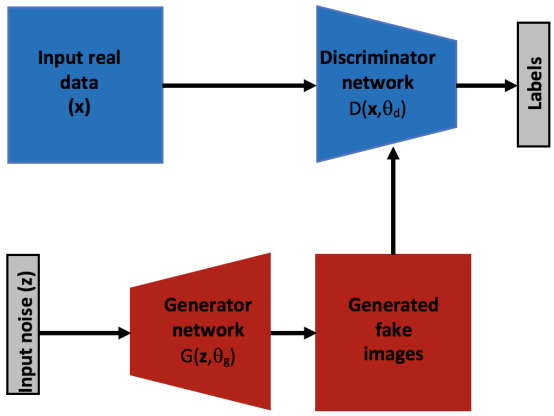

Figure 2.7: Illustration of the structure of a general purpose Generative Adverserial Network (GAN).

two blocks are trained alternately in several steps where the ideal outcome of the training process is a discriminator that assigns a probability of 50% to both real and fake data. In other words, after convergence the generator should be able to generate realistic data from random input.

Since the original paper, many contributions participated in enhancing the capabilities of GANs via use of more powerful multilayer architectures as the backbones of the network [114] (*e.g.* pretrained convolutional networks for the discriminator and deconvolutional networks, that learn upsampling filters for the generator). Some of the successful applications of GANs include: text to image synthesis (where the input to the network is a textual description of the image to be rendered [115]), image super resolution where the GAN generates a realistic high resolution image from a lower resolution input [94], image inpainting where the role of GANs is to fill holes of missing information from an input image [149] and texture synthesis where GANs are used to synthesize realistic textures from input noise [10].

2.1.5 Multilayer network training

As discussed in the previous sections, the success of the various multilayer architectures largely depends on the success of their learning process. While neural networks usually rely on an unsupervised pretraining step first, as described in Section 2.1.1, they are usually followed by the most widely used training strategy for multilayer architectures, which is fully supervised. The training procedure is usually based on

error back propagation using gradient descent. Gradient descent is widely used in training multilayer architectures for its simplicity. It relies on minimizing a smooth error function, $E(\boldsymbol{w})$, following an iterative procedure defined as

$$\mathbf{w}_k = \mathbf{w}_{k-1} - \alpha \frac{\partial E(\mathbf{w})}{\partial \mathbf{w}}, \tag{2.11}$$

where $\mathbf{w}$ represents the network's parameters, α is the learning rate that may control the speed of convergence and $\frac{\partial \mathbf{E(w)}}{\partial \mathbf{w}}$ is the error gradient calculated over the training set. This simple gradient descent method is especially suitable for training multilayer networks thanks to the use of the chain rule for back propagating and calculating the error derivative with respect to various network's parameters at different layers. While back propagation dates back a number of years [16,146], it was popularized in the context of multilayer architectures [125]. In practice, stochastic gradient descent is used [2], which consists of approximating the error gradient over the entire training set from successive relatively small subsets.

One of the main problems of the gradient descent algorithm is the choice of the learning rate, α. A learning rate that is too small leads to slow convergence, while a large learning rate can lead to overshooting or fluctuation around the optimum. Therefore, several approaches were proposed to further improve the simple stochastic gradient descent optimization method. The simplest method, referred to as stochastic gradient descent with momentum [137], keeps track of the update amount from one iteration to another and gives momentum to the learning process by pushing the update further if the gradient keeps pointing to the same direction from one time step to another as defined in,

$$\mathbf{w}_k = \mathbf{w}_{k-1} - \alpha \frac{\partial E(\mathbf{w})}{\partial \mathbf{w}} - \gamma (\frac{\partial E(\mathbf{w})}{\partial \mathbf{w}})_{t-1}, \tag{2.12}$$

with γ controlling the momentum. Another simple method involves setting the learning rate in a decreasing fashion according to a fixed schedule, but this is far from ideal given that this schedule has to be pre-set ahead of the training process and is completely independent from the data. Other more involved methods (*e.g.* Adagrad [34], Adadelta [152], Adam [86]) suggest adapting the learning rate during

training to each parameter, w_i, being updated, by performing smaller updates on frequently changing parameters and larger updates on infrequent ones. A detailed comparison between the different versions of these algorithms can be found elsewhere [124].

The major shortcoming of training using gradient descent, as well as its variants, is the need for large amounts of labeled data. One way to deal with this difficulty is to resort to unsupervised learning. A popular unsupervised method used in training some shallow ConvNet architectures is based on the Predictive Sparse Decomposition (PSD) method [85]. Predictive Sparse Decomposition learns an overcomplete set of filters whose combination can be used to reconstruct an image. This method is especially suitable for learning the parameters of a convolutional architecture, as the algorithm is designed to learn basis functions that reconstruct an image patchwise. Specifically, Predictive Sparse Decomposition (PSD) builds on sparse coding algorithms that attempts to find an efficient representation, Y, of an input signal, X, via a linear combination with a basis set, B. Formally, the problem of sparse coding is broadly formulated as a minimization problem defined as,

$$L(X, Y; B) = ||X - BY||_2^2. \tag{2.13}$$

PSD adapts the idea of sparse coding in a convolutional framework by minimizing a reconstruction error defined as,

$$L(X, Y; B) = ||X - BY||_2^2 + \lambda||Y||_1 + \alpha||Y - F(X; G, W, D)||_2^2 \tag{2.14}$$

where $F(X; G, W, D) = G\ \tanh(WX + D)$ and W, D and G are weights, biases and gains (or normalization factors) of the network, respectively. By minimizing the loss function defined in equation 2.14, the algorithm learns a representation, Y, that reconstructs the input patch, X, while being similar to the predicted representation F. The learned representation will also be sparse owing to the second term of the equation. In practice, the error is minimized in two alternating steps where parameters, (B, G, W, D), are fixed and minimization is performed over Y. Then,

the representation Y is fixed while minimizing over the other parameters. Notably, PSD is applied in a patchwise procedure where each set of parameters, (G, W, D), is learned from the reconstruction of a different patch from an input image. In other words, a different set of kernels is learned by focusing the reconstruction on different parts of the input images.

2.1.6 A word on transfer learning

One of the unexpected benefits of training multilayer architecture is the surprising adaptability of the learned features across different datasets and even different tasks. Examples include using networks trained with ImageNet for recognition on: other object recognition datasets such as Caltech-101 [38] (*e.g.* [96, 154]), other recognitions tasks such as texture recognition (*e.g.* [25]), other applications such as object detection (*e.g.* [53]) and even to video based tasks, such as video action recognition (*e.g.* [41, 134, 144]).

The adaptability of features extracted with multilayer architectures across different datasets and tasks, can be attributed to their hierarchical nature where the representations progress from being simple and local to abstract and global. Thus, features extracted at lower levels of the hierarchy tend to be common across different tasks thereby making multilayer architectures more amenable to transfer learning.

不一定，折中的方案是，先fine tuning higher layer，然后fine tuning the entire network

A systematic exploration of the intriguing transferability of features across different networks and tasks revealed several good practices to take into account in consideration of transfer learning [150]. First, ~~it was shown that fine tuning higher layers only, led to systematically better performance when compared to fine tuning the entire network.~~ Second, this research demonstrated that the more different the tasks are the less efficient transfer learning becomes. Third, and more surprisingly, it was found that even after fine tuning the network's performance under the initial task is not particularly hampered.

Recently, several emerging efforts attempt to enforce a networks' transfer learning capabilities even further by casting the learning problem as a sequential two step procedure, *e.g.* [3, 127]. First, a so called rapid learning step is performed where a network is optimized for a specific task as is usually done. Second, the network

parameters are further updated in a global learning step that attempts to minimize an error across different tasks.

2.2 Spatial convolutional networks 空间卷积网络

In theory, convolutional networks can be applied to data of arbitrary dimensions. Their two dimensional instantiations are well suited to the structure of single images and therefore have received considerable attention in computer vision. With the availability of large scale datasets and powerful computers for training, the vision community has recently seen a surge in the use of ConvNets for various applications. This section describes the most prominent 2D ConvNet architectures that introduced relatively novel components to the original LeNet described in Section 2.1.3.

2.2.1 Key architectures in the recent evolution of ConvNets

The work that rekindled interest in ConvNet architectures was Krishevsky's AlexNet [88]. AlexNet was able to achieve record breaking object recognition results on the ImageNet dataset. It consisted of eight layers in total, 5 convolutional and 3 fully connected, as depicted in Figure 2.8.

AlexNet introduced several architectural design decisions that allowed for efficient training of the network using standard stochastic gradient descent. In particular, four important contributions were key to the success of AlexNet. First, AlexNet considered the use of the ReLU nonlinearity instead of the saturating nonlinearites, such as sigmoids, that were used in previous state-of-the-art ConvNet architectures (*e.g.* LeNet [91]). The use of the ReLU diminished the problem of vanishing gradient and led to faster training. Second, noting the fact that the last fully connected layers in a network contain the largest number of parameters, AlexNet used dropout, first introduced in the context of neural networks [136], to reduce the problem of overfitting. Dropout, as implemented in AlexNet, consists in randomly dropping (*i.e.* setting to zero) a given percentage of a layer's parameters. This technique allows for training a slightly different architecture at each pass and artificially reducing the number of parameters to be learned at each pass, which ultimately helps break

correlations between units and thereby combats overfitting. Third, AlexNet relied on data augmentation to improve the network's ability to learn invariant representations. For example, the network was trained not only on the original images in the training set, but also on variations generated by randomly shifting and reflecting the training images. Finally, AlexNet also relied on several techniques to make the training process converge faster, such as the use momentum and a scheduled learning rate decrease whereby the learning rate is decreased every time the learning stagnates.

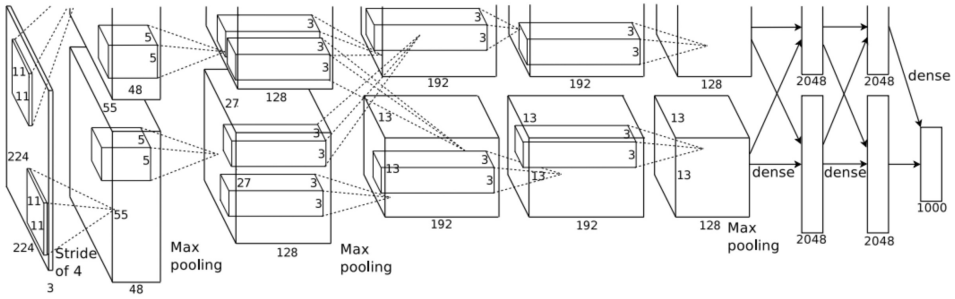

Figure 2.8: AlexNet architecture. Notably, although the depiction suggests a two stream architecture, it was in fact a single stream architecture and this depiction only reflects the fact that AlexNet was trained in parallel on 2 different GPUs. Figure reproduced from [88].

The advent of AlexNet led to a spurt in the number of papers trying to understand what the network is learning either via visualization, as done in the so called DeConvNet [154], or via systematic explorations of various architectures [22, 23]. One of the direct results of these explorations was the realization that deeper networks can achieve even better results as first demonstrated in the 19 layer deep VGG-Net [135]. VGG-Net achieves its depth by simply stacking more layers while following the standard practices introduced with AlexNet (*e.g.* reliance on the ReLU nonlinearity and data augmentation techniques for better training). The main novelty presented in VGG-Net was the use of filters with smaller spatial extent (*i.e.* 3×3 filters throughout the network instead of *e.g.* 11×11 filters used in AlexNet), which allowed for an increase in depth without dramatically increasing the number of parameters that the network needs to learn. Notably, while using smaller filters, VGG-Net required far more filters per layer.

VGG-Net was the first and simplest of many deep ConvNet architectures that followed AlexNet. A deeper architecture, commonly known as GoogLeNet, with 22 layers was proposed later [138]. While being deeper than VGG-Net, GoogLeNet requires far fewer parameters thanks to the use of the so called inception module, shown in Figure 2.9(a), as a building block. In an inception module convolution operations at various scales and spatial pooling happen in parallel. The module is also augmented with 1×1 convolutions (*i.e.* cross-channel pooling) that serve the purpose of dimensionality reduction to avoid or attenuate redundant filters, while keeping the network's size manageable. This cross-channel pooling idea was motivated by the findings of a previous work known as the Network in Network (NiN) [96], which disucssed the large redundancies in the learned networks. Stacking many inception modules led to the now widely used GoogLeNet architecture depicted in Figure 2.9(b).

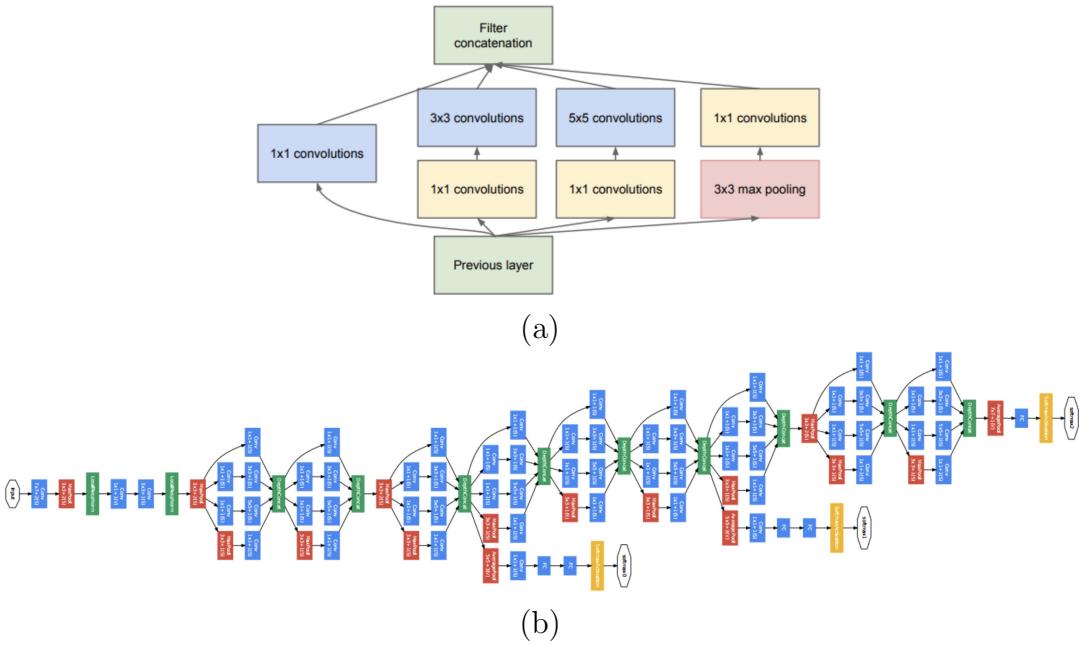

(a)

(b)

Figure 2.9: GoogLeNet architecture. (a) A typical inception module showing operations that happen sequentially and in parallel. (b) Illustration of a typical "inception" architecture that consists of stacking many inception modules. Figure reproduced from [138]

GoogLeNet was the first network to stray away from the strategy of simply stacking convolutional and pooling layers and it was soon followed by one of the deepest architectures to date, known as ResNet [64], that also proposed a novel

architecture with over 150 layers. ResNet stands for Residual Network where the main contribution lies in its reliance on residual learning. In particular, ResNet is built such that each layer learns an incremental transformation, $F(x)$, on top of the input, x, according to

$$H(x) = F(x) + x, \tag{2.15}$$

instead of learning the transformation $H(x)$ directly as done in other standard ConvNet architectures. This residual learning is achieved via use of skip connections, illustrated in Figure 2.10(a), that connect components of different layers with an identity mapping. Direct propagation of the signal, x, combats the vanishing gradient problem during back propagation and thereby enables the training of very deep architectures.

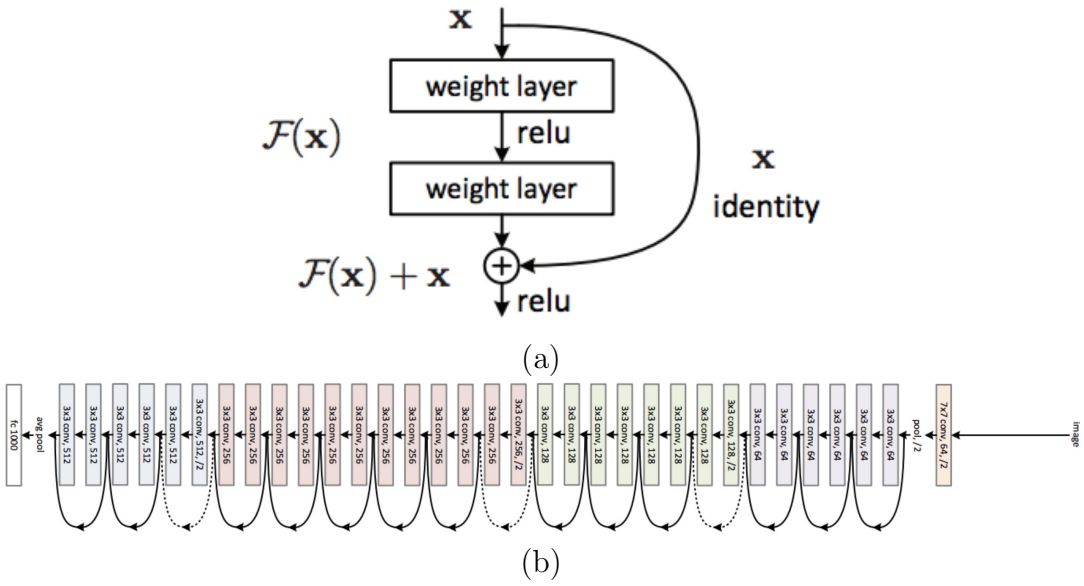

Figure 2.10: ResNet architecture. (a) A residual module. (b) Illustration of a typical ResNet architecture that consists of stacking many residual modules. Figure reproduced from [64].

A recent, closely related network building on the success of ResNet is the so called DenseNet [72], which pushes the idea of residual connections even further. In DenseNet, every layer is connected, via skip connections, to all subsequent layers of a dense block as illustrated in Figure 2.11. Specifically, a dense block connects all layers with feature maps of the same size (*i.e.* blocks between spatial pooling layers).

Different from ResNet, DenseNet does not add feature maps from a previous layer, (2.15), but instead concatenates features maps such that the network learns a new representation according to

$$H(x_l) = F(x_{l-1}, ..., x_1, x_0). \tag{2.16}$$

The authors claim that this strategy allows DenseNet to use fewer filters at each layer since possible redundant information is avoided by pushing features extracted at one layer to other layers higher up in the hierarchy. Importantly, these deep skip connections allow for better gradient flow given that lower layers have more direct access to the loss function. Using this simple idea allowed DenseNet to compete with other deep architectures, such as ResNet, while requiring fewer parameters and incurring less overfitting.

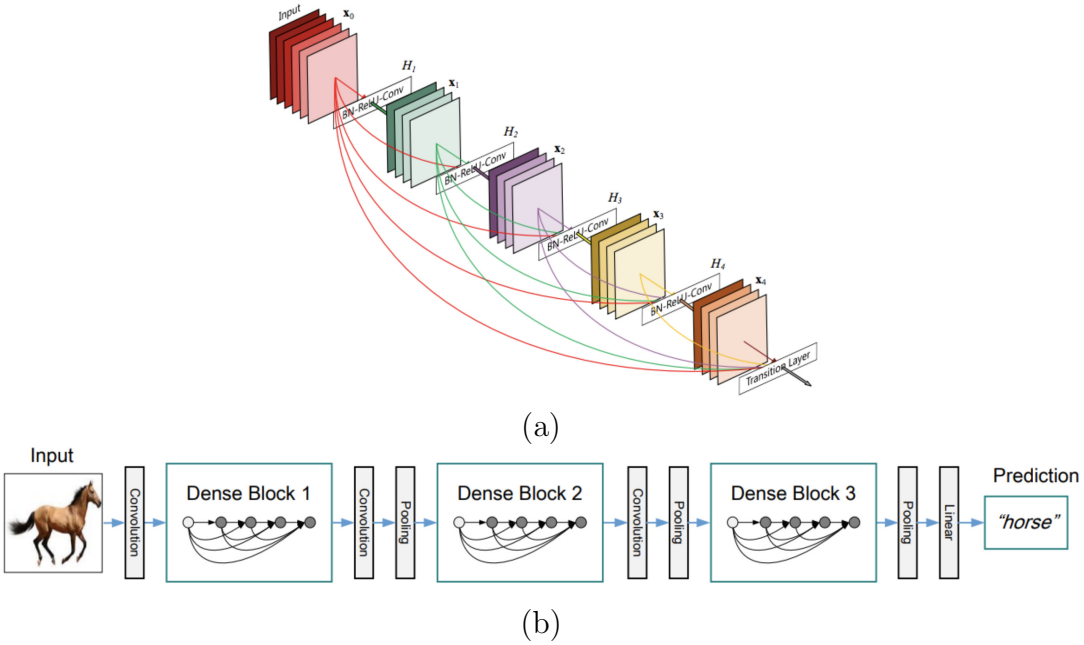

Figure 2.11: DenseNet architecture. (a) A dense module. (b) Illustration of a typical DenseNet architecture that consists of stacking many dense modules. Figure reproduced from [72].

2.2.2 Toward ConvNet invariance

One of the challenges of using ConvNets is the requirement of very large datasets to learn all the underlying parameters. Even large scale datasets such as Ima-

geNet [126], with over a million images, is considered too small for training certain deep architectures. One way to cope with the large dataset requirement is to artificially augment the dataset by altering the images via random flipping, rotation and jittering, for example. The major advantage of these augmentations is that the resulting networks become more invariant to various transformations. In fact, this technique was one of the main reasons behind the large success of AlexNet. Therefore, beyond methods altering the network's architecture for easier training, as discussed in the previous section, other work aims at introducing novel building blocks that yield better training. Specifically, networks discussed under this section introduce novel blocks that incorporate learning invariant representation directly from the raw data.

A prominent ConvNet that explicitly tackles invariance maximization is the Spatial Transformer Network (STN) [76]. In particular, this network makes use of a novel learned module that increased invariance to unimportant spatial transformations, *e.g.* those that result from varying viewpoint during object recognition. The module is comprised of three submodules: A localization net, a grid generator and a sampler, as shown in Figure 2.12(a). The operations performed can be summarized in three steps. First, the localization net, which is usually a small 2 layer neural network, takes a feature map, U, as input and learns transformation parameters, θ, from this input. For example, the transformation, $\mathcal{T}_\theta$, can be defined as a general affine transformation allowing the network to learn translations, scalings, rotations and shears. Second, given the transformation parameters and an output grid of pre-defined size, $H \times W$, the grid generator calculates for each output coordinate, (x_i^t, y_i^t), the corresponding coordinates, (x_i^s, y_i^s), that should be sampled from the input, U, according to

$$\begin{pmatrix} x_i^s \\ y_i^s \end{pmatrix} = \begin{bmatrix} \theta_{11} & \theta_{12} & \theta_{13} \\ \theta_{21} & \theta_{22} & \theta_{23} \end{bmatrix} \begin{pmatrix} x_i^t \\ y_i^t \\ 1 \end{pmatrix}. \tag{2.17}$$

Finally, the sampler takes the feature map, U, and the sampled grid and interpolates the pixels values, (x_i^s, y_i^s), to populate the output feature map, V, at locations (x_i^t, y_i^t)

as illustrated in Figure 2.12(b). Adding such modules at each layer of any ConvNet architecture allows it to learn various transformations adaptively from the input to increase its invariance and thereby improve its accuracy.

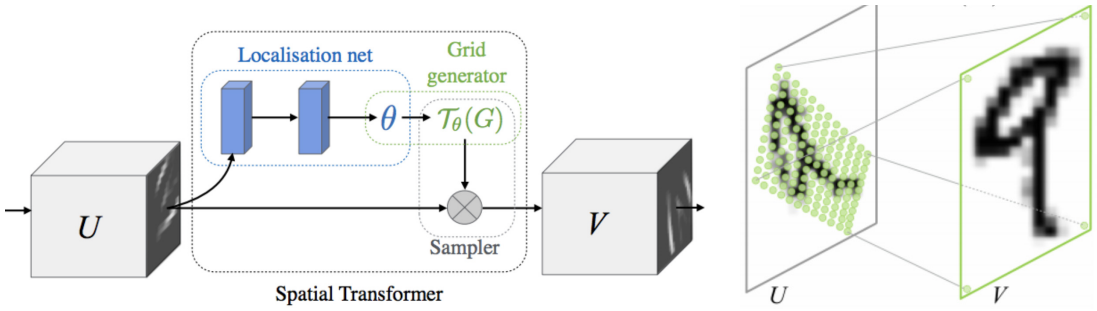

(a) (b)

Figure 2.12: Spatial Transformer Networks operations. (a) Depictions of a Spatial Transformer module, a typical transformation operation is illustrated in (b). Figure reproduced from [76].

With the same goal of enhancing the geometric transformation modeling capability of ConvNets, two contemporary approaches, known as Deformable ConvNet [29] and Active ConvNet [78], introduce a flexible convolutional block. The basic idea in these approaches is to eschew the use of rigid windows during convolution in favor of learning Regions of Interest (RoI) over which convolutions are performed. This idea is akin to what is done by the localization network and the grid generator of a Spatial Transformer module. To determine the RoIs at each layer, the convolutional block is modified such that it learns offsets from the initial rigid convolution window. Specifically, starting from the standard definition of a convolution operation over a rigid window given by

$$y(p) = \sum_{p_n \in R} w(p_n)\, x(p - p_n), \tag{2.18}$$

where R is the region over which convolution is performed, p_n are the pixel locations within the region R and $w(p_n)$ are the corresponding filter weights, an new term is added to include offsets according to

$$y(p) = \sum_{p_n \in R} w(p_n)\, x(p - p_n - \triangle p_n), \tag{2.19}$$

where $\triangle p_n$ are the offsets and now the final convolution step will be performed over a deformed window instead of the traditional rigid $n \times n$ window. To learn the offsets, $\triangle p_n$, the convolutional block of Deformable ConvNets is modified such that it includes a new submodule whose role is to learn the offsets as depicted in Figure 2.13. Different from Spatial Transformer Networks that alternately learn the submodule parameters and the network weights, Deformable ConvNets learn the weights and offsets concurrently, thus making it faster and easier to deploy in various architectures.

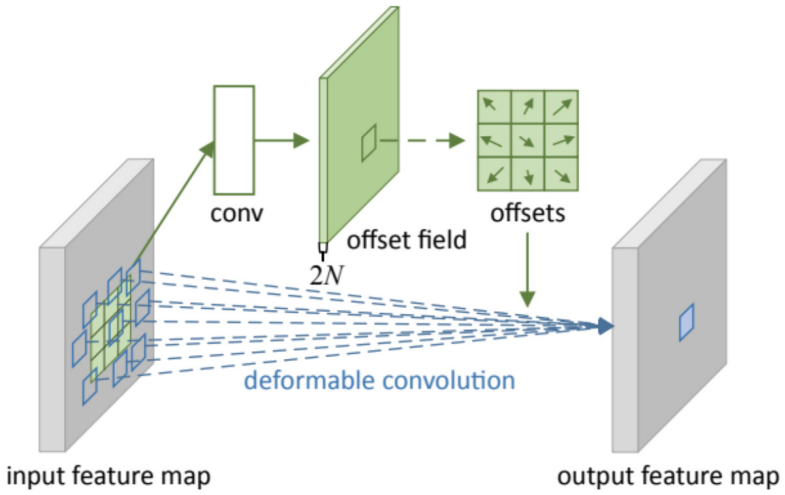

Figure 2.13: Deformable or active convolution. Starting from a fixed window size the network learns offsets via a small subnetwork (shown in the top part of the figure in green) and finally performs convolution on a deformed window. Figure reproduced from [29].

2.2.3 Toward ConvNet localization

Beyond simple classification tasks, such as object recognition, recently ConvNets have been excelling at tasks that require accurate localization as well, such as semantic segmentation and object detection. Among the most successful networks for semantic segmentation is the so called Fully Convolutional Network (FCN) [98]. As the name implies, FCN does not make use of fully connected layers explicitly but instead casts them as convolutional layers whose receptive fields cover the entire underlying feature map. Importantly, the network learns an upsampling or deconvolution filter that recovers the full resolution of the image at the last layer

as depicted in Figure 2.14. In FCN, the segmentation is achieved by casting the problem as a dense pixelwise classification. In other words, a softmax layer is attached to each pixel and segmentation is achieved by grouping pixels that belong to the same class. Notably, it was reported in this work that using features from lower layers of the architecture in the upsampling step plays an important role. It allowed for more accurate segmentation given that lower layer features tend to capture finer grained details, which are far more important for a segmentation task compared to classification. An alternative to learning a deconvolution filter, relies on using atrou or dilated convolutions [24], *i.e.* upsampled sparse filters, which helps recovering higher resolution feature maps while keeping the number of parameters to be learned manageable.

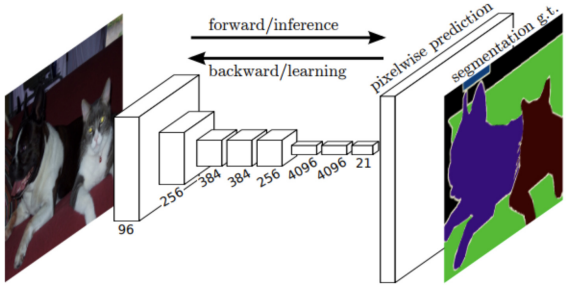

Figure 2.14: Fully Convolutional Network. After upsampling to recover the image full resolution at the last layer, each pixel is classified using a softmax to finally generate the segments. Figure reproduced from [98].

When it comes to object localization, one of the earliest approaches within the ConvNet framework is known as Region CNN or R-CNN. This network combined a region proposal method with a ConvNet architecture [53]. Although R-CNN was built around simple ideas, it yielded state-of-the-art object detection results. In particular, R-CNN first uses an off-the-shelf algorithm for region proposals (*e.g.* selective search [140]) to detect potential regions that may contain an object. These regions are then warped to match the default input size of the employed ConvNet and fed into a ConvNet for feature extraction. Finally, each region's features are classified with an SVM and refined in a post processing step via non-maximum suppression.

In its naive version, R-CNN simply used ConvNets as a feature extractor. However, its ground breaking results led to improvements that take more advantage

of ConvNets' powerful representation. Examples include, Fast R-CNN [52], Faster R-CNN [116] and Mask R-CNN [61]. Fast R-CNN, proposes propagating the independently computed region proposals through the network to extract their corresponding regions in the last feature map layer. This technique, avoids costly passes through the network for each region extracted from the image. In addition, Fast R-CNN avoids heavy post-processing steps by changing the last layer of the network such that it learns both object classes and refined bounding box coordinates. Importantly, in both R-CNN and Fast R-CNN the detection bottleneck lies in the region proposal step that is done outside of the ConvNet paradigm.

Faster R-CNN pushes the use of ConvNets even further by adding a sub-module (or sub-network), called Region Proposal Network (RPN), after the last convolutional layer of a ConvNet. An RPN module enables the network to learn the region proposals as part of the network optimization. Specifically, RPN is designed as a small ConvNet consisting of a convolutional layer and a small fully connected layer and two outputs that return potential object positions and objectness scores (*i.e.* probability of belonging to an object class). The entire network's training is achieved following an iterative two step procedure. First, the network is optimized for region proposal extraction using the RPN unit. Second, keeping the extracted region proposals fixed, the network is finetuned for object classification and final object bounding box position. More recently, mask R-CNN was introduced to augment faster R-CNN with the ability to segment the detected regions yielding tight masks around the detected objects. To this end, mask R-CNN adds a segmentation branch to the classification and bounding box regression branches of faster R-CNN. In particular, the new branch is implemented as a small FCN that is optimized for classifying pixels in any bounding box to one of two classes; foreground or background. Figure 2.15 illustrates the differences and progress from simple R-CNN to mask R-CNN.

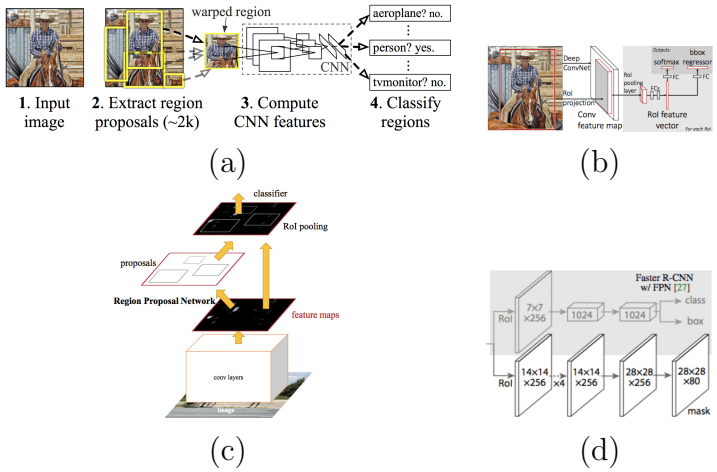

Figure 2.15: Progress of prominent region proposal networks. (a) Structure of the original R-CNN. Figure reproduced from [53]. (b) Structure of Fast R-CNN. Figure reproduced from [52]. (c) Structure of Faster R-CNN. Figure reproduced from [116].(d) Structure of Mask R-CNN. Figure reproduced from [61].

2.3 Spatiotemporal convolutional networks

The significant performance boost brought to various image based applications via use of ConvNets, as discussed in Section 2.2, sparked interest in extending 2D spatial ConvNets to 3D spatiotemporal ConvNets for video analysis. Generally, the various spatiotemporal architectures proposed in the literature have simply tried to extend 2D architectures from the spatial domain, (x, y), into the temporal domain, (x, y, t). In the realm of training based spatiotemporal ConvNets, there are three different architectural design decisions that stand out: LSTM based (*e.g.* [33, 112]), 3D (*e.g.* [84, 139]) and Two-Stream ConvNets (*e.g.* [43, 134]), which will be described in this section.

2.3.1 LSTM based spatiotemporal ConvNet

LSTM based spatiotemporal ConvNets, *e.g.* [33, 112], were some of the early attempts to extend 2D networks to spacetime processing. Their operations can be summarized in three steps as shown in Figure 2.16. First, each frame is processed with a 2D network and feature vectors are extracted from their last layer. Second, these features, from different time steps, are then used as input to LSTMs that

produce temporal outcomes, y_t. Third, these outcomes are then either averaged or linearly combined and passed to a softmax classifier for final prediction.

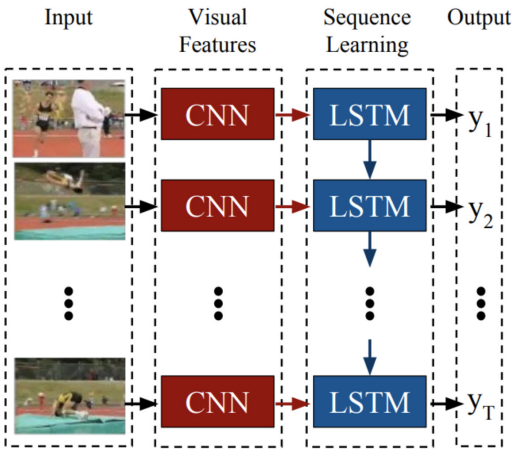

Figure 2.16: Sample LSTM based spatiotemporal ConvNet. In this network the input consists of consecutive frames from a video stream. Figure reproduced from [33].

The goal of LSTM based ConvNets is to progressively integrate temporal information while not being restricted to a strict input size (temporally). One of the benefits of such an architecture is equipping the network with the ability to produce variable size text descriptions (*i.e.* a task at which LSTMs excel), as done in [33]. However, while LSTMs can capture global motion relationships, they may fail at capturing finer grained motion patterns. In addition, these models are usually larger, need more data and are therefore hard to train. To date, excepting cases where video and text analysis are being integrated (*e.g.* [33]), LSTMs generally have seen limited success in spatiotemporal image analysis.

2.3.2 3D ConvNet

The second prominent type of spatiotemporal networks provides the most straightforward generalization of standard 2D ConvNet processing to image spacetime. It works directly with temporal streams of RGB images and operates on these images via application of learned 3D, (x, y, t), convolutional filters. Some of the early attempts at this form of generalization use filters that extend into the temporal domain with very shallow networks [80] or only at the first convolutional layer [84].

When using 3D convolutions at the first layer only, small tap spatiotemporal filters are applied on each 3 or 4 consecutive frames. To capture longer range motions multiple such streams are used in parallel and the hierarchy that results from stacking such streams increases the network's temporal receptive field. However, because spatiotemporal filtering is limited to the first layer only, this approach did not yield a dramatic improvement over a naive frame based application of 2D ConvNets. A stronger generalization is provided by the now widely used C3D network, that uses 3D convolution and pooling operations at all layers [139]. The direct generalization of C3D from a 2D to a 3D architecture entails a great increase in the number of parameters to be learned, which is compensated for by using very limited space-time support at all layers (*i.e.* $3 \times 3 \times 3$ convolutions). A recent, slightly different, approach proposes integration of temporal filtering by modifying the ResNet architecture [64] to become a Temporal ResNet (T-ResNet) [42]. In particular, T-ResNet augments the residual units (shown in Figure 2.10(a)) with a $1 \times 1 \times T$ filter that applies one dimensional learned filtering operations along the temporal dimension.

Ultimately, the goal of such 3D ConvNet architectures is to directly integrate spacetime filtering throughout the model in order to capture both appearance and motion information at the same time. The main downside of these approaches is the entailed increase in the number of their parameters.

2.3.3 Two-Stream ConvNet

The third type of spatiotemporal architecture relies on a two-stream design. The standard Two-Stream architecture [134], depicted in Figure 2.17, operates in two parallel pathways, one for processing appearance and the other for motion by analogy with the two-stream hypothesis in the study of biological vision systems [55]. Input to the appearance pathway are RGB images; input to the motion path are stacks of optical flow fields. Essentially, each stream is processed separately with fairly standard 2D ConvNet architectures. Separate classification is performed by each pathway, with late fusion used to achieve the final result. The various improvements over the original two stream network follow from the same underlying idea while using various baseline architectures for the individual streams (*e.g.* [43, 143, 144]) or

proposing different ways of connecting the two streams (*e.g.* [40, 41, 43]). Notably, recent work known as I3D [20], proposes use of both 3D filtering and Two-Stream architectures via use of 3D convolutions on both streams. However, the authors do not present compelling arguments to support the need for a redundant optical flow stream in addition to 3D filtering, beyond the fact that the network achieves slightly better results on benchmark action recognition datasets.

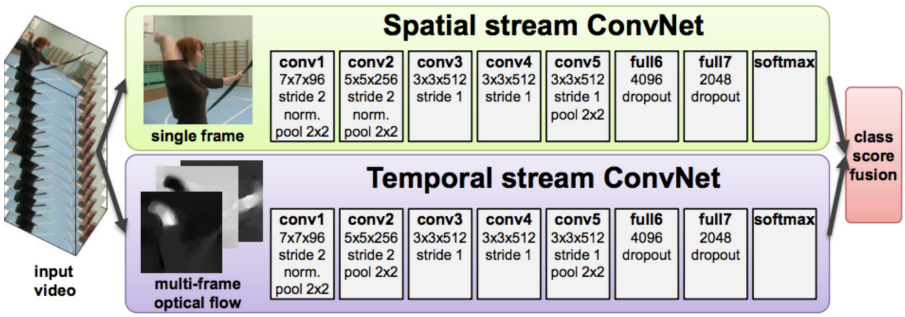

Figure 2.17: The original Two-Stream Network. The network takes as input RGB frames and stacks of optical flow. Figure reproduced from [134].

Overall, Two-Stream ConvNets support the separation of appearance and motion information for understanding spatiotemporal content. Significantly, this architecture seems to be the most popular among spatiotemporal ConvNets as its variations led to state-of-the-art results on various action recognition benchmarks (*e.g.* [40, 41, 43, 144]).

2.4 Overall discussion

Multilayer representations have always played an important role in computer vision. In fact, even standard widely used hand crafted features such as SIFT [99] can be seen as a shallow multilayer representation, which loosely speaking consists of a convolutional layer followed by pooling operations. Moreover, pre-ConvNet state-of-the-art recognition systems typically followed hand-crafted feature extraction with (learned) encodings followed by spatially organized pooling and a learned classifier (*e.g.* [39]), which also is a multilayer representational approach. Modern multilayer architectures push the idea of hierarchical data representation deeper while typically eschewing hand designed features in favor of learning based approaches. When it

comes to computer vision applications, the specific architecture of ConvNets makes them one of the most attractive architectures.

Overall, while the literature tackling multilayer networks is very large where each faction advocates the benefits of one architecture over another, some common "best practices" have emerged. Prominent examples include: the reliance of most architectures on four common building blocks (*i.e.* convolution, rectification, normalization and pooling), the importance of deep architectures with small support convolutional kernels to enable abstraction with a manageable number of parameters, residual connections to combat challenges in error gradient propagation during learning. More generally, the literature agrees on the key point that good representations of input data are hierarchical, as previously noted in several contributions [119].

Importantly, while these networks achieve competitive results in many computer vision applications, their main shortcomings remain: the limited understanding of the exact nature of the learned representation, the reliance on massive training datasets, the lack of ability to support precise performance bounds and the lack of clarity regarding the choice of the networks hyper parameters. These choices include the filters sizes, choice of nonlinearities, pooling functions and parameters as well as the number of layers and architectures themselves. Motivations behind several of these choices, in the context of ConvNets' building block, are discussed in the next chapter.

Chapter 3

Understanding ConvNets Building Blocks

In the light of the plethora of unanswered questions in the ConvNets area, this chapter investigates the role and significance of each layer of processing in a typical convolutional network. Toward this end, the most prominent efforts tackling these questions are reviewed. In particular, the modeling of the various ConvNet components will be presented both from theoretical and biological perspectives. The presentation of each component ends with a discussion that summarizes our current level of understanding.

3.1 The convolutional layer

The convolutional layer is, arguably, one of the most important steps in ConvNet architectures. Basically, convolution is a linear, shift invariant operation that consists of performing local weighted combination across the input signal. Depending on the set of weights chosen (*i.e.* the chosen point spread function) different properties of the input signal are revealed. In the frequency domain, the correlate of the point spread function is the modulation function that tells how the frequency components of the input are modified through scaling and phase shifting. Therefore, it is of paramount importance to select the right kernels to capture the most salient and important information contained in the input signal that allows for making

strong inferences about the content of the signal. This section discusses some of the different ways to approach the kernel selection step.

3.1.1 Biological perspective

Neurophysiological evidence for hierarchical processing in the mamalian visual cortex provides an underlying inspiration for spatial and spatiotemporal ConvNets. In particular, research that hypothesized a cascade of simple and complex cells that progressively extract more abstract attributes of the visual input [74] has been of particular importance. At the very earliest stages of processing in the visual cortex, the simple cells were shown capable of detecting primitive features such as oriented gratings, bars and edges, with more complicated tunings emerging at subsequent stages.

A popular choice for modeling the described properties of cortical simple cells is a set of oriented Gabor filters or Gaussian derivatives at various scales. More generally, filters selected at this level of processing typically are oriented bandpass filters. Many decades later most biological models still rely on the same set of simple cells at the initial layers of the hierarchy [5, 48, 79, 117, 130, 131]. In fact, these same Gabor kernels are also extended to the chromatic [155] and temporal [79] domains to account for color and motion sensitive neurons, respectively.

Matters become more subtle, however, when it comes to representing cells at higher areas of the visual cortex and most contributions building on Hubel and Wiesel's work strive to find an appropriate representation for these areas. The HMAX model is one of the most well known models tackling this issue [117]. The main idea of the HMAX model is that filters at higher layers of the hierarchy are obtained through the combination of filters from previous layers such that neurons at higher layers respond to co-activations of previous neurons. This method ultimately should allow the model to respond to more and more complex patterns at higher layers as illustrated in Figure 3.1. This approach relates nicely to the Hebbian theory stating that "cells that fire together, wire together" [65].

Another hallmark of the HMAX model is the assumption that learning comes into play in order to recognize across various viewpoints of similar visual sequences.

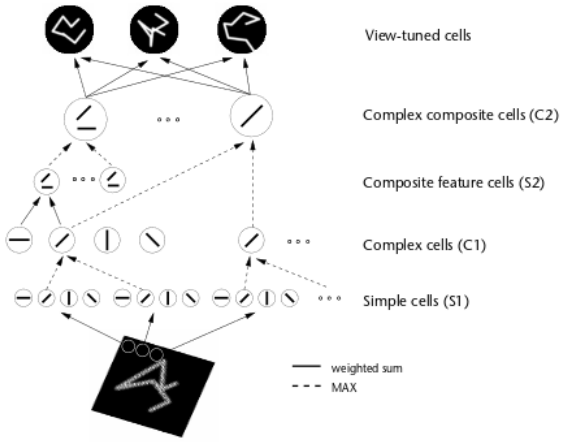

Figure 3.1: Illustration of the HMAX Model. This model consists of a hierarchy of cells with alternating simple (S) and complex (C) cells. Filtering operations happen at the level of the S cells. It is shown in this figure that simple cells at the initial layer ($S1$) detect simple oriented bars (*i.e.* through the use of oriented Gabor filters). On the other hand, simple cells at higher layers ($S2$) respond to filtering with templates that are combinations of filters used at the previous ($S1$) layer such that cells at higher layers in the hierarchy detect more complex shapes than oriented bars. Complex composite cells (C1, C2) intervene between the layers of simple cells to aggregate similarly tuned cells across spatial position and thereby achieve a degree of shift invariance. Figure reproduced from [117].

Direct extensions of this work thereafter explicitly introduce learning to model filters at higher layers. Among the most successful such approaches is the biologically motivated network introduced by Serre *et al.* [131] that attempts to model the processes taking place at the initial layers of the visual cortex with a network made of 4 layers where simple (S) and complex (C) cells alternate as illustrated in Figure 3.2. It is seen that each simple cell is directly followed by a complex cell such that the overall structure of the network can be summarizes as $S1 \rightarrow C1 \rightarrow S2 \rightarrow C2$. In this network convolutions take place at the level of the $S1$ and $S2$ units. While the $S1$ units rely on $2D$ oriented Gabor filters, the kernels used at the second layer are based on a learning component. This choice is motivated by biological evidence suggesting that learning occurs at the higher layers of the cortex [130], although there also is evidence that learning plays a role at earlier layers of the visual cortex [11]. In this case, the learning process corresponds to selecting a random set of $n \times n \times l$ patches, $\mathbf{P}_i$, from a training set at the $C1$ layer, where n is the spatial extent of the patch and l corresponds to the number of orientations. The $S2$ layer feature

maps are obtained by performing template matching between the $C1$ features in each scale and the set of learned patches $\mathbf{P}_i$ at all orientations simultaneously.

A direct extension to this work exists for video processing [79]. The kernels used for video processing are designed to mimic the behavior of cells in the dorsal stream. In this case, $S1$ units involve convolutions with 3D oriented filters. In particular, third order Gaussian derivative filters are used owing to their nice separability properties and a similar learning process is adopted to select convolutional kernels for the $S2$ and $S3$ units.

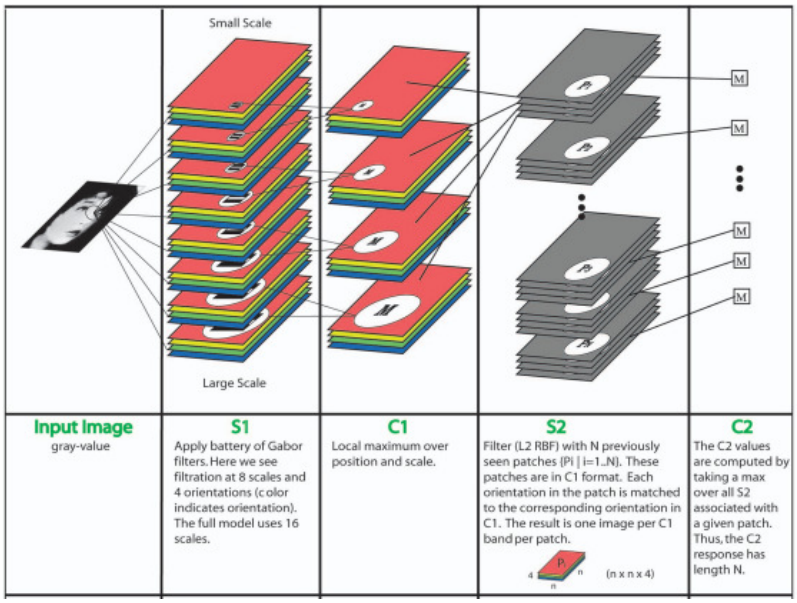

Figure 3.2: The Network Architecture Proposed by Serre *et al.* Similarly to the HMAX model [117], it consists of alternating simple and complex cells such that the overall architecture of the proposed networks can be summarized as $S1 \rightarrow C1 \rightarrow S2 \rightarrow C2$. However, as opposed to the HMAX model, templates used at the level of the S2 cells are explicitly learned from a training set such that this layer detects complex objects (*i.e.* when trained with an object recognition dataset). The details of the process are summarized in the second row of the figure. Figure reproduced from [131].

Many variations of the above underlying ideas have been proposed, including various learning strategies at higher layers [145, 147], wavelet based filters [71], different feature sparsification strategies [73, 110, 147] and optimizations of filter parameters [107, 147].

Another related, although somewhat different, train of thoughts suggest that there exist more complex cells at higher levels of the hierarchy that are dedicated

to capturing intermediate shape representation, *e.g.* curvatures [120, 121]. While the HMAX class of models propose modeling shapes via compositions of feature types from previous layers, these investigations propose an approach that directly models hypercomplex cells (also referred to as endstopped cells) without resorting to learning. In particular, models falling within this paradigm model hypercomplex cells via combination of simple and complex cells to generate new cells that are able to maximally respond to curvatures of different degrees and signs as well as different shapes at different locations. In suggesting that hypercomplex cells subserve curvature calculations, this work builds on earlier work suggesting similar functionality, *e.g.* [32].

Yet another body of research, advocates that the hierarchical processing (termed $Filter \rightarrow Rectify \rightarrow Filter$) that takes place in the visual cortex deals progressively with higher-order image structures [5, 48, 108]. It is therefore advocated that the same set of kernels present at the first layer (*i.e.* oriented bandpass filters) are repeated at higher layers. However, the processing at each layer reveals different properties of the input signal given that the same set of kernels now operate on different input obtained from a previous layer. Therefore, features extracted at successive layers progress from simple and local to abstract and global while capturing higher order statistics. In addition, joint statistics are also accounted for through the combination of layerwise responses across various scales and orientations.

Discussion

The ability of human visual cortex in recognizing the world while being invariant to various changes has been the driving force of many researchers in this field. Although, several approaches and theories have been proposed to model the different layers of the visual cortex, a common thread across these efforts is the presence of hierarchical processing that splits the vision task into smaller pieces. However, while most models agree on the choice of the set of kernels at the initial layers, motivated by the seminal work of Hubel and Wiesel [74], modeling areas responsible for recognizing more abstract features seems to be more intricate and controversial. Also, these biologically plausible models, typically leave open critical questions regarding

the theoretical basis of their design decisions. This shortcoming applies to more theoretically driven models as well, as will be discussed in the next section.

3.1.2 Theoretical perspective

More theoretically driven approaches are usually inspired from biology but strive to inject more theoretical justifications into their models. These methods usually vary depending on their kernel selection strategy.

One way of looking at the kernel selection problem is to consider that objects in the natural world are a collection of a set of primitive shapes and thereby adopt a shape based solution [45–47]. In this case, the proposed algorithms start by finding the most primitive shapes in an image (*i.e.* oriented edges) using a bank of oriented Gabor filters. Using these edges, or more generally parts, the algorithm proceeds by finding potential combinations of parts in the next layers by looking at increasingly bigger neighborhoods around each part. Basically, every time a new image is presented to the network, votes are collected about the presence of other part types in the direct neighborhood of a given part in the previous layer. After all images present in the training set are seen by the network, each layer of the network is constructed using combinations of parts from the previous layer. The choice of the combinations is based on the probabilities learned during the unsupervised training. In reality, such a shape based approach is more of a proof of concept where only lower layers of the hierarchy can be learned in such an unsupervised way, whereas higher layers are learned using category specific images as illustrated in Figure 3.3. Therefore, a good representation of an object can be obtained in higher layers only if the network saw examples from that object class alone. However, because of this constraint, such an algorithm cannot be reasonably deployed on more challenging datasets with objects from different categories that it had not previously seen.

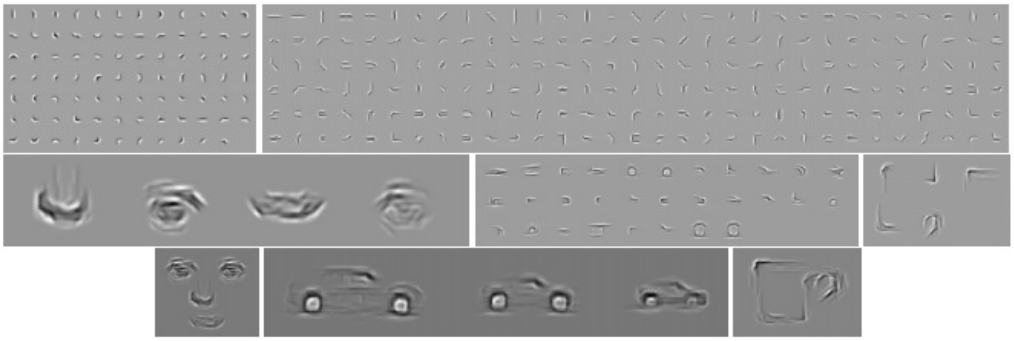

Figure 3.3: Sample Parts Learned by the Multilayer Architecture Proposed by Fidler *et al*. **1st row (left-to-right):** Layer 2 and layer 3 sample parts**. 2nd and 3rd rows:** Layer 4 and layer 5 parts learned using faces, cars, and mugs. Figure reproduced from [47].

Another outlook on the kernel selection process is based on the observation that many training based convolutional networks learn redundant filters. Moreover, many of the learned filters at the first few layers of those networks resemble oriented band pass filters; *e.g*. see Figure 3.8. Therefore, several recent investigations aim at injecting priors into their network design with a specific focus on the convolutional filter selection. One approach proposes learning layerwise filters over a basis set of 2D derivative operators [75] as illustrated in Figure 3.4. While this method uses a fixed basis set of filters, it relies on supervised learning to linearly combine the filters in the basis at each layer to yield the effective layerwise filters and it is therefore dataset dependent. Nonetheless, using a basis set of filters and learning combinations aligns well with biological models, such as HMAX [117] and its successors (*e.g*. [79, 131]), and simplifies the networks' architecture, while maintaining interpretability. Also, as learning is one of the bottlenecks of modern ConvNets, using a basis set also eases this process by tremendously decreasing the number of parameters to be learned. For these reasons such approaches are gaining popularity in the most recent literature [28, 75, 100, 148, 158].

Interestingly, a common thread across these recent efforts is the aim of reducing redundant kernels with a particular focus on modeling rotational invariance (although it is not necessarily a property of biological vision). The focus on rotation is motivated by the observation that, often, learned filters are rotated versions of one another. For example, one effort targeted learning of rotational equivariance

by training over a set of circular harmonics [148]. Alternatively, other approaches attempt to hard encode rotation invariance by changing the network structure itself such that for each learned filter a set of corresponding rotated versions are automatically generated either directly based on a predefined set of orientations, *e.g.* [158], or by convolving each learned filter with a basis set of oriented Gabor filters [100].

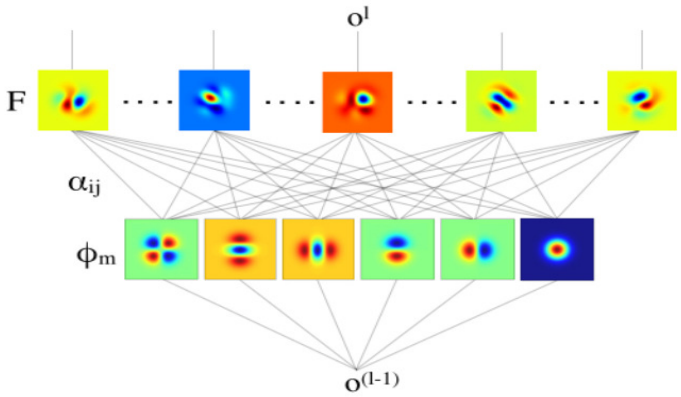

Figure 3.4: An Illustration the Receptive Fields CNN (also known as RFNN). In this network, the filters used at all layers are built (via learning) as a linear combination of the basis filter set ϕ_m, which is a set n^{th} order Gaussian derivatives. Instead of learning the kernel parameters of the filters, this network learns the parameters α_{ij} used to linearly combine the filters in the basis set. Figure reproduced from [75].

Other approaches push the idea of injecting priors into their network design even further by fully hand crafting their network via casting the kernel selection problem as an invariance maximization problem based on group theory, *e.g.* [15, 28, 113]. For example, kernels can be chosen such that they maximize invariances to small deformations and translations for texture recognition [15] or to maximize rotation invariance for object recognition [113].

Arguably, the scattering transform network (ScatNet) has one of the most rigorous mathematical definitions to date [15]. The construction of scattering transforms starts from the assertion that a good image representation should be invariant to small, local deformations and various transformation groups depending on the task at hand. The kernels used in this method are a set of dilated and rotated wavelets ψ_λ where λ is the frequency location of the wavelet and it is defined as $\lambda = 2^{-j}r$ where 2^{-j} represents the dilation and r represents the rotation. The network is constructed by a hierarchy of convolutions using various wavelets centered around

different frequencies, as well as various nonlinearities as discussed in the next section. The frequency locations of the employed kernels are chosen to be smaller at each layer. The entire process is summarized in Figure 3.5.

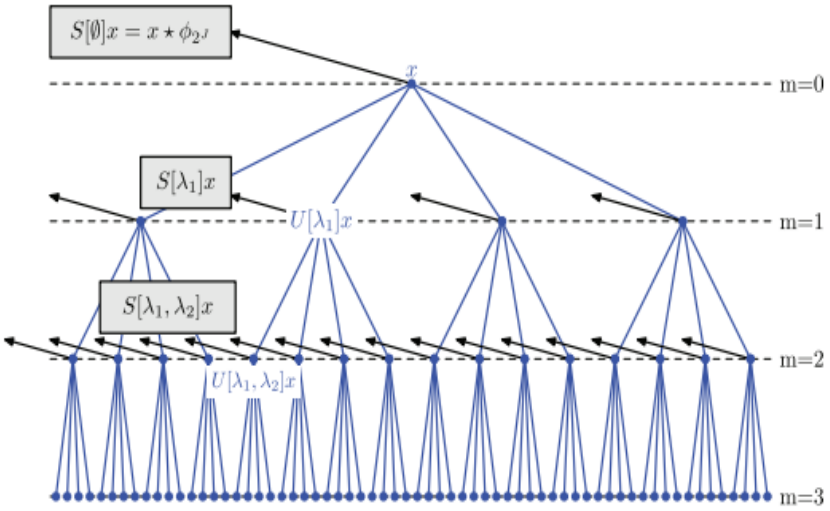

Figure 3.5: Scattering Transform Network. In this network, the scattering transform $S[\lambda]x$ proposed in [15] is applied repeatedly at each layer m on all the outputs $U[\lambda_i]x$ from a previous layer. Essentially, the outputs of each layer go through the same transform over and over again, however, the transform targets a different effective frequency at each layer and thereby extracts novel information at each layer. In this figure, an instantiation of the network with $m = 3$ layers is depicted as an illustration. Figure reproduced from [15].

A related ConvNet, dubbed SOE-Net, was proposed for spacetime image analysis [60]. SOE-Net relies on a vocabulary of theory motivated, analytically defined filters. In particular, its convolutional block relies on a basis set of 3D oriented Gaussian derivative filters that are repeatedly applied while following a frequency decreasing path similar to ScatNet as illustrated in Figure 3.6. In this case, however, the network design is cast in terms of spatiotemporal orientation analysis and invariance is enforced via a multiscale instantiation of the used basis set.

Loosely speaking both SOE-Net and ScatNet fall under the $Filter \rightarrow Rectify \rightarrow Filter$ paradigm advocated by some biologically based models [5]. Because these network are based on a rigorous mathematical analysis, they also take into account the frequency content of the signal as it is processed in each layer. One of the direct results of this design is the ability to make theory driven decisions regarding the number of layers used in the network. In particular, given that outputs of the

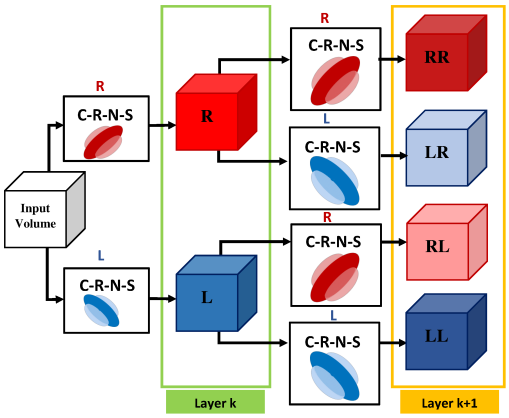

Figure 3.6: SOE-Net Architecture. Local spatiotemporal features at various orientations are extracted with an initial processing layer, $\mathcal{L}_k$. C-R-N-S indicate Convolution, Rectification, Normalization and Spatiotemporal pooling, while R and L indicate rightward vs. leftward filtered data, resp., with symbol strings (*e.g.* LR) indicating multiple filterings. A network with only 2 filters (*i.e.* 2 orientations) is shown for illustration. Each of the feature maps at layer $\mathcal{L}_k$ is treated as a new separate signal and fed back to layer $\mathcal{L}_{k+1}$ to be convolved with the same set of filters but at a different effective resolution due to spatiotemporal pooling. Figure reproduced from [60].

different layers of the network are calculated using a frequency decreasing path, the signal eventually decays. Hence, the iterations are stopped once there is little energy left in the signal. Further, through its choice of filters that admit a finite basis set (Gaussian derivatives), SOE-Net can analytically specify the number of orientations required.

Another simple, yet powerful, outlook on the kernel selection process relies on pre-fixed filters learned using PCA [21]. In this approach, it is argued that PCA can be viewed as the simplest class of auto-encoders that minimize reconstruction error. The filters are simply learned using PCA on the entire training dataset. In particular, for each pixel in each image X_i, a patch of size $k_1 \times k_2$ is taken and subjected to a de-meaning operation to yield a set of patches $\bar{X}_i$. A collection of such overlapped patches from each image is stacked together to form the volume $X = [\bar{X}_1, \bar{X}_2, ..., \bar{X}_N]$. The filters used correspond to the first L_1 principal eigenvectors of XX^T. These vectors are reshaped to form kernels W_l of size $k_1 \times k_2$ and convolved with each input image X_i to obtain feature maps I_i^l. The same procedure is repeated for higher layers of the network.

Compared to ScatNet [15] and SOE-Net [60], the PCA approach work is much less mathematically involved and relies more on learning. However, it is worth highlighting that the most basic form of auto-encoder was able to achieve respectable results on several tasks including face recognition, texture recognition and object recognition. A closely related approach also relies on unsupervised kernel selection as learned via k-means clustering [35]. Once again, although such an approach does not yield state-of-the art results compared to standard learning based architectures it is worthy of note that it still is competitive even on heavily researched datasets such as MNIST [91]. More generally, the effectiveness of such purely unsupervised approaches suggest that there is non-trivial information that can be leveraged simply from the inherent statistics of the data.

3.1.2.1 Optimal number of kernels

As previously mentioned, the biggest bottleneck of multilayer architectures is the learning process that requires massive amounts of training data mainly due to the large number of parameters to be learned. Therefore, it is of paramount importance to carefully design the network's architecture and decide on the number of kernels at each layer. Unfortunately, even hand-crafted ConvNets usually resort to a random selection of the number of kernels (*e.g.* [15, 21, 45, 79, 113, 131]). One exception among the previously discussed analytically defined ConvNets is SOE-Net, which as previously mentioned, specifies the number of filters analytically owing to its used of a finite basis set (*i.e.* oriented Gaussian derivatives).

The recent methods that suggest the use of basis sets to reduce the number of kernels at each layer [28, 75] offer an elegant way of tackling this issue although the choice of the set of filters and the number of filters in the set is largely based on empirical considerations. The other most prominent approaches tackling this issue aim at optimizing the network architecture during the training process. A simple approach to deal with this optimization problem, referred to as optimal brain damage [92], is to start from a reasonable architecture and progressively delete small magnitude parameters whose deletion does not negatively affect the training process. A more sophisticated approach [44] is based on the Indian Buffet Process [59]. The

optimal number of filters is determined by training a network to minimize a loss function $\mathcal{L}$ that is a combination of three objectives

$$\mathcal{L} = \sum_{l=1}^{L} \mathcal{L}_{task}(.) + \sum_{l=1}^{L_{conv}} \mathcal{L}_{conv}(.) + \sum_{l=L_{conv}+1}^{L} \mathcal{L}_{fc}(.), \tag{3.1}$$

where L_{conv} is the number of convolutional layers and L is the total number of layers. In (3.1), $\mathcal{L}_{fc}$ and $\mathcal{L}_{conv}$ are the unsupervised loss functions of the fully connected and convolutional layers, respectively. Their role is to minimize reconstruction errors and are trained using unlabeled data. In contrast, $\mathcal{L}_{task}$ is a supervised loss function designed for the target task and is trained to maximize classification accuracy using labeled training data. Therefore, the number of filters K in each layer is tuned by minimizing both a reconstruction error and a task related loss function. This approach allows the proposed network to use both labeled and unlabeled data.

In practice, the three loss functions are minimized alternatively. First, the filter parameters $W^{(l)}$ are fixed and the number of filters $K^{(l)}$ is learned with a Grow-And-Prune (GAP) algorithm using all available training data (i.e. labeled and unlabeled). Second, the filter parameters are updated by minimizing the task specific loss function using the labeled training data. The GAP algorithm can be described as a two way greedy algorithm. The forward pass increases the number of filters. The backward pass reduces the network size by removing redundant filters.

Discussion

Overall, most theoretically driven approaches to convolutional kernel selection aim at introducing priors into their hierarchical representations with the ultimate goal of reducing the need for massive training. In doing so, these methods either rely on maximizing invariances through methods grounded in group theory or rely on combinations over basis sets. Interestingly, similar to more biologically inspired instantiations, it also is commonly observed that there is a pronounced tendency to model early layers with filters that have the appearance of oriented bandpass filters. However, the choice for higher layers' kernels remains an open critical question.

3.2 Rectification

Multilayer networks are typically highly nonlinear and rectification is, usually, the first stage of processing that introduces nonlinearities to the model. Rectification refers to applying a pointwise nonlinearity (also known as an activation function) to the output of the convolutional layer. Use of this term borrows from signal processing, wherein rectification refers to conversion from alternating to direct current. It is another processing step that finds motivation both from biological and theoretical point views. Computational neuroscientists introduce the rectification step in an effort to find the appropriate models that explain best the neuroscientific data at hand. On the other hand, machine learning researchers use rectification to obtain models that learn faster and better. Interestingly, both streams of research tend to agree, not only on the need for rectification, but they are also converging to the same type of rectification.

3.2.1 Biological perspective

From a biological perspective, rectification nonlinearities are usually introduced into the computational models of neurons in order to explain their firing rates as a function of the input [31]. A fairly well accepted model for biological neuron's firing rate in general is referred to as the *Leaky Integrate and Fire* (LIF) [31]. This model explains that the incoming signal to any neuron has to exceed a certain threshold in order for the cell to fire. Research investigating the cells in the visual cortex in particular also relies on a similar model, referred to as half wave rectification [66, 74, 109].

Notably, Hubel and Wiesel's seminal work already presented evidence that simple cells include nonlinear processing in terms of half wave rectification following on linear filtering [74]. As previously mentioned in Section 3.1, the linear operator itself can be considered as a convolution operation. It is known that, depending on the input signal, convolution can give rise to either positive or negative outputs. However, in reality cells' firing rates are by definition positive. This is the reason why Hubel and Wiesel suggested a nonlinearity in the form of a clipping operation that

only takes into account the positive responses. More in line with the LIF model, other research suggested a slightly different half wave rectification in which the clipping operation happens based on a certain threshold (*i.e.* other than zero) [109]. Another more complete model also took into account the possible negative responses that may arise from the filtering operation [66,67]. In this case, the author suggested a two-path half wave rectification where the positive and negative incoming signals are clipped separately and carried in two separate paths. Also, in order to deal with the negative responses both signals are followed by a pointwise squaring operation and the rectification is therefore dubbed half-squaring (although biological neurons do not necessarily share this property). In this model the cells are regarded as energy mechanisms of opposite phases that encode both the positive and negative outputs.

Discussion

Notably, these biologically motivated models of neuronal activation functions have become common practice in today's convolutional network algorithms and are, in part, responsible for much of their success as will be discussed next.

3.2.2 Theoretical perspective

From a theoretical perspective, rectification is usually introduced by machine learning researchers for two main reasons. First, it is used to increase the discriminating power of the extracted features by allowing the network to learn more complex functions. Second, it allows for controlling the numerical representation of the data for faster learning. Historically, multilayer networks relied on pointwise sigmoidal nonlinearities using either the logistic nonlinearity or the hyperbolic tangent [91]. Although the logistic function is more biologically plausible given that it does not have a negative output, the hyperbolic tangent was more often used given that it has better properties for learning such as a steady state around 0 (See Figures 3.7 (a) and (b), respectively). To account for the negative parts of the hyperbolic tangent activation function it is usually followed by a modulus operation (also referred to as *Absolute Value Rectification* AVR) [77]. However, recently the *Rectified Linear Unit* (ReLU), first introduced by Nair *et al.* [111], quickly became the default rectification

Relu能防止过拟合？

nonlinearity in many fields (*e.g.* [103]) and particularly computer vision ever since its first successful application on the ImageNet dataset [88]. It was shown in [88] that the ReLU plays a key role against overfitting and expediting the training procedure, even while leading to better performance compared to traditional sigmoidal rectification functions.

Mathematically, ReLU is defined as follows,

$$f(y_i) = max(0, y_i) \tag{3.2}$$

and is depicted in Figure 3.7 (c). The ReLU operator has two main desirable properties for any learning based network. First, ReLU does not saturate for positive input given that its derivative is 1 for positive input. This property makes ReLU particularly attractive since it removes the problem of vanishing gradients usually present in networks relying on sigmoidal nonlinearities. Second, given that ReLU sets the output to 0 when the input is negative, it introduces sparsity, which has the benefit of faster training and better classification accuracy. In fact, for improved classification it is usually desirable to have linearly separable features and sparse representations are usually more readily separable [54]. However, the hard 0 saturation on negative input comes with its own risks. Here, there are two complementary concerns. First, due to the hard zero activation some parts of the network may never be trained if the paths to these parts were never activated. Second, in a degenerate case where all units at a given layer have a negative input, back propagation might fail and this will lead to a situation that resembles the vanishing gradient problem. Because of these potential issues many improvements to the ReLU nonlinearity have been proposed to deal better with the case of negative outputs while keeping the advantages of ReLU.

Variations of the ReLU activation function include the *Leaky Rectified Linear Unit* (LReLU) [103] and its closely related *Parametric Rectified Linear Unit* (PReLU) [63] that are mathematically defined as

$$f(y_i) = max(0, y_i) + a_i min(0, y_i) \tag{3.3}$$

and depicted in Figure 3.7 (d). In LRelu a_i is a fixed value, whereas it is learned in PReLU. LReLU was initially introduced to avoid zero gradients during back propagation but did not improve the results of the tested networks significantly. Also, it heavily relied on cross validation experimentation in the selection of the parameter a_i. In contrast, PReLU optimizes the value of this parameter during training, which leads to a bigger boost in performance. Notably, one of the most important results of PReLU is the fact that early layers in the network tended to learn a higher value for the parameters a_i, whereas that number is almost negligible for higher layers in the network's hierarchy. The authors speculate that this result could be due to the nature of the filters learned at different layers. In particular, since first layer kernels are usually oriented bandpass like filters both parts of the response are kept as they represent a potentially significant difference in the incoming signal. On the other hand, kernels at higher layers are tuned to detect specific objects and are trained to be more invariant.

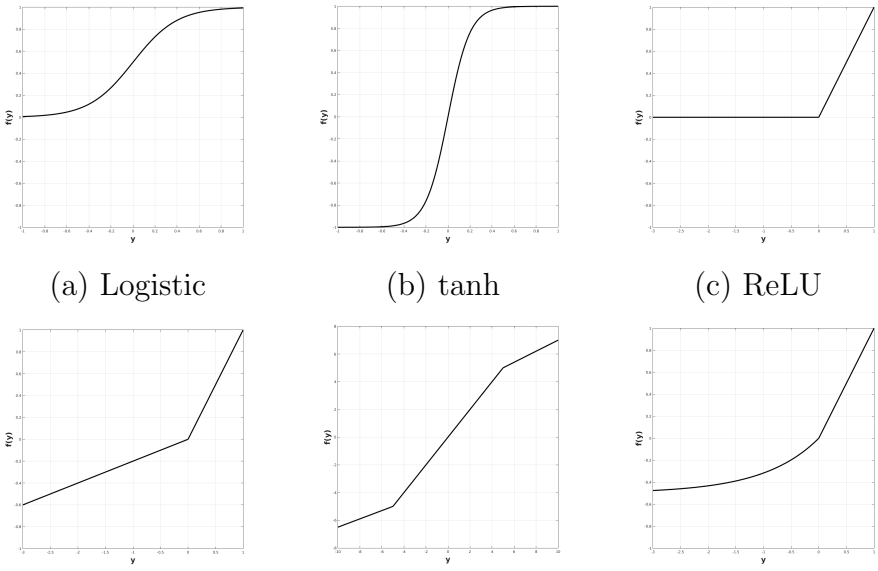

(a) Logistic (b) tanh (c) ReLU

(d) LReLU/PReLU (e) SReLU (f) EReLU

Figure 3.7: Nonlinear Rectification Functions Used in the Multilayer Networks Literature.

Interestingly, another rectification function, dubbed *Concatenated Rectified Linear Unit* (CReLU), was proposed based on similar observations [132]. In that case, the authors propose CReLU starting from the observation that kernels learned at

the initial layers of most ConvNets tend to form negatively correlated pairs (*i.e.* filters that are 180 degrees out of phase) as shown in Figure 3.8. This observation implies that the negative responses eliminated by the ReLU nonlinearity are replaced by learning kernels of opposite phase. By replacing ReLU with CReLU, the authors were able to demonstrate that a network designed to encode a two path rectification leads to a better performance, while reducing the number of parameters to be learned through removing redundancies.

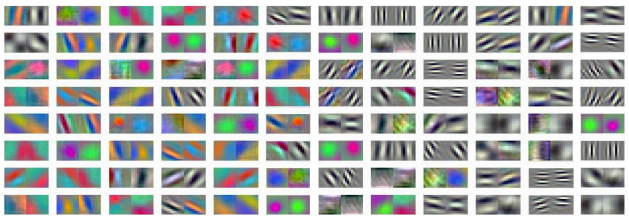

Figure 3.8: Visualization of Conv1 Filters Learned by AlexNet Trained on ImageNet Dataset. Figure reproduced from [132].

Other variation in the ReLU family include: the the *S-shaped Rectified Linear Unit* (SReLU) [82], defined as

$$f(y_i) = \begin{cases} t_i^r + a_i^r(y_i - t_i^r) & if\ y_i \geq t_i^r \\ y_i & if\ t_i^r > y_i > t_i^l \\ t_i^l + a_i^l(y_i - t_i^l) & if\ y_i \leq t_i^l \end{cases} \tag{3.4}$$

and depicted in Figure 3.7 (e), which was introduced to allow networks to learn more nonlinear transformations. It consists of three piecewise linear functions with 4 learnable parameters. The main downside of SReLU is that it introduces several parameters to learn (*i.e.* particularly if the parameters are not shared among several channels), which makes learning more complex. This concern is especially true given that a bad initialization of those parameters might impair the learning. Yet another variant is the *Exponential Linear Unit* (ELU) [26], defined as

$$f(y_i) = \begin{cases} y_i & if\ x > 0 \\ \alpha(exp(y_i) - 1) & if\ x \leq 0 \end{cases} \tag{3.5}$$

and depicted in Figure 3.7 (f), which is motivated by a desire to increase invariance to noise by forcing the signal to saturate to a value controlled by a variable α for negative inputs. A common thread across all variations in the ReLU family is that the negative input should be taken into account as well and dealt with appropriately.

Another outlook on the choice of the rectification nonlinearity is presented in the Scattering Network [15]. As previously mentioned in Section 3.1, ScatNet is handcrafted with the main goal of increasing invariance of the representation to various transformations. Since it broadly relies on Wavelets in the convolutional layer it is invariant to small deformations; however, it remains covariant to translation. Therefore, the authors rely on an integral operation defined as

$$S[\lambda]x(u) = ||x \star \psi_\lambda||_1 = \int |x \star \psi_\lambda(u)|\, du \tag{3.6}$$

and implemented as average pooling, to add a level of shift invariance. Hence, in anticipation of the subsequent pooling operation that can drive the response towards zero, *i.e.* in the case where positive and negative responses cancel each other, the $\mathbf{L}_1(\mathbb{R}^2)$ norm operator is used in the rectification step to make all responses positive. Once again, it is worth noting here that traditional ConvNets that relied on the hyperbolic tangent activation function also used a similar AVR rectification to handle negative outputs [77, 91]. Also, more biologically motivated models, such as the half-squaring rectification [66, 67], relied on pointwise squaring of the signal to deal with negative responses. This squaring operation also allows for reasoning about the responses in terms of energy mechanisms. Interestingly, one of the recent more theory driven convolutional networks [60] also proposed a a two path rectification strategy defined as

$$\begin{aligned} E^+(\mathbf{x};\theta_i,\sigma_j) &= (\max[C(\mathbf{x};\theta_i,\sigma_j),0])^2 \\ E^-(\mathbf{x};\theta_i,\sigma_j) &= (\min[C(\mathbf{x};\theta_i,\sigma_j),0])^2 \end{aligned}, \tag{3.7}$$

where $C(\mathbf{x};\theta_i,\sigma_j)$ is the output from the convolution operation. This rectification strategy combines the idea of keeping both phases of the filtered signal and pointwise squaring and thereby allows for conservation the signals magnitude and phase while

considering the resulting signal in terms of spectral energy.

Discussion

Interestingly, the broad class of ReLU nonlinearities clearly became the most popular choice for the rectification stage from a theoretical perspective. Notably, the choice of completely neglecting the negative inputs (*i.e.* as done in ReLU) seems to be more questionable as evidenced by the many contributions proposing alternatives to this choice [26, 63, 82, 103, 132]. It is also important to compare the behavior of the ReLU with AVR rectification used in ScatNet [15] and older ConvNet architectures [77]. While AVR preserves the energy information but erases the phase information, ReLU on the other hand keeps the phase information in some sense, by retaining the positive parts of the signal only; however, it does not preserve the energy as it throws away half of the signal. Significantly, methods that try to preserve both (*e.g.* CReLU [132] and the use of (3.7) in SOE-Net [60]) were able to achieve better performances across several tasks, and such methods are also in consensus with biological findings [66].

3.3 Normalization

As previously mentioned, multilayer architectures are highly nonlinear due to the cascade of nonlinear operations that take place in these networks. In addition to the rectification nonlinearity discussed in the previous section, normalization is another nonlinear block of processing that plays a significant role in ConvNet architectures. The most widely used form of normalization used in ConvNets is the so called *Divisive Normalization* or DN (also known as local response normalization). This section sheds light on the role of the normalization step and describes how it corrects for some of the shortcomings of the previous two blocks of processing (*i.e.* Convolution and Rectification). Once again the role of normalization will be discussed both from biological and theoretical perspectives.

3.3.1 Biological perspective

Normalization was proposed early on by neurophysiologists to explain the phenomenon of light adaptation in the retina [13] and was later extended to explain the nonlinear properties of neurons in the mammalian visual cortex [66]. Indeed, from a biological point of view, the need for a normalization step stems from two main observations [66, 67]. First, although cells responses were proven to be stimulus specific [74], it was also shown that cell responses can inhibit one another and that there exists a phenomenon of cross-orientation suppression, where the response of a neuron to its preferred stimuli is attenuated if it is superimposed with another ineffective stimuli [14, 19, 67]. Neither the linear models (*i.e.* in the convolution step) nor the different forms of rectification discussed in the previous section, such as half-wave rectification proposed by computational neuroscientists, explain this cross-orientation suppression and inhibition behavior. Second, while cell responses are known to saturate at high contrast, a model relying only on convolution and unbounded rectifiers, such as ReLU, will have values that keep increasing with increasing contrast. These two observations suggested the need for a step that discounts the responses of other stimuli in order to keep the specificity of each cell and make it contrast invariant while explaining other inhibition behaviors of cells.

One popular model to deal with these issues includes a divisive normalization block described mathematically as follows

$$\bar{E}_i = \frac{E_i}{\sigma^2 + \sum_j E_j}, \tag{3.8}$$

where E_i is the output of a squared, half wave rectified convolution operation, pooled over a set of orientations and scales j and σ^2 is a saturation constant that can be chosen based on either one of two adaptation mechanisms [66]. In the first case, it could be a different value for each cell learned from the cell's response history. The second possibility is to derive it from the statistics of the responses of all cells. This divisive normalization scheme discards information about magnitude of the contrast in favor of encoding the underlying image pattern in terms of relative contrast across the input responses, E_j, in the normalization operation, (3.8). Use of this model

seemed to provide a good fit to neuron responses of mammalian visual cortex [67]. It was also shown that it explains well the cross-orientation suppression phenomenon as well [14].

Discussion

Interestingly, most of the studies investigating the role of divisive normalization show that neuronal models including it fit well the recorded data (*e.g.* [14,19,66,67]). Indeed, more recent studies suggest that divisive normalization could also explain the phenomenon of adaptation in IT cortex where the neural responses decrease with stimulus repetition (*e.g.* [83]). Moreover, the suggested prevalence of divisive normalization in several areas of the cortex lead to the hypothesis that Divisive Normalization can be seen as a canonical operation of the mammalian visual cortex similar to the operation of convolution [19].

3.3.2 Theoretical perspective

From a theoretical perspective, normalization has been explained as being a method of achieving efficient coding when representing natural images [102]. In that work, the normalization step was motivated by findings regarding the statistics of natural images [102] that are known to be highly correlated and for containing very redundant information. In light of these findings, the normalization step was introduced with the goal of finding a representation that minimizes statistical dependencies in images. To achieve this goal a popular derivation discussed thoroughly in [101, 102] starts by representing images using a statistical model based on a Gaussian Scale Mixture. Using this model and an objective function whose role is to minimize dependencies, a nonlinearity is derived in the form of

$$r_i = \frac{x_i - \sum_j a_j x_j}{\sqrt{b + \sum_k c_j (x_j - \sum_k a_k x_k)^2}} \tag{3.9}$$

where x_i and r_i are the input and output images, respectively, while b, a_i and c_i are parameters of the divisive normalization that can be learned from a training set. Notably, there exists a direct relationship between the definition of the divisive

normalization introduced to deal with redundancies and high order dependencies in natural images, (3.9), and that suggested to best fit neuron responses in the visual cortex, (3.8). In particular, with a change of variable where we set $y_i = x_i - \sum_j a_j x_j$, we see that the two equations are related, subject to the square root difference, by an elementwise operation, (*i.e.* squaring, with $E_i = y_i^2$), and thereby both models achieve the goal of maximizing independence while satisfying neuroscientific observations.

Another way of looking at normalization in ConvNets in particular is to consider it as a way of enforcing local competition between features [77, 91], similar to the one taking place in biological neurons. This competition can be enforced between adjacent features within a feature map through subtractive normalization or between feature maps through divisive normalization operating at the same spatial locations across feature maps. Alternatively, divisive normalization can be seen as a way of minimizing sensitivity to multiplicative contrast variation [60]. It was also found, on deeper network architectures, that divisive normalization was helpful in increasing the generalization power of a network [88].

More recent ConvNets rely on what is referred to as *batch normalization* [129]. Batch normalization is another kind of divisive normalization that takes into account a batch of the training data to learn normalization parameters (*i.e.* the mean and variance in equation (3.10)) and it also introduces new hyperparameters, $\gamma^{(k)}$and $\beta^{(k)}$, to control the amount of normalization needed at each layer.

Batch normalization can be summarized in two steps. First, at any layer with a d-dimensional input $x = (x^{(1)} ... x^{(d)})$, each scalar feature is independently normalized according to

$$\widehat{x}^{(k)} = \frac{x^{(k)} - E[x^{(k)}]}{\sqrt{Var[x^{(k)}]}}, \tag{3.10}$$

with $E[x^{(k)}]$ being the mini-batch mean calculated as $E[x^{(k)}] = \frac{1}{m}\sum_{i=1}^{m} x_i$ over the m samples of the mini-batch, and $Var[x^{(k)}]$ is the variance of the same mini-batch calculated as $Var[x^{(k)}] = \frac{1}{m}\sum_{i=1}^{m}(x_i - E[x^{(k)}])^2$. Second, the output of the normalization in equation (3.10) is subject to a linear transformation such that the

final output of the proposed batch normalization block is given by $y^{(k)} = \gamma^{(k)}\widehat{x}^{(k)} + \beta^{(k)}$, with $\gamma^{(k)}$and $\beta^{(k)}$ being hyperparameters to be learned during training.

The first step in batch normalization aims at fixing the means and variances of the inputs at each layer. However, since that normalization strategy can change or limit what a layer can represent, the second linear transformation step is included to maintain the network's representational power. For example, if the original distribution at the input was already optimal, then the network can restore it by learning an identity mapping. Therefore, the normalized inputs, $\widehat{x}^{(k)}$, can be thought of as being inputs to a linear block added at each layer of a network.

Batch normalization was first introduced as an improvement to traditional divisive normalization with the ultimate goal of reducing the problem of *internal covariate shift*, which refers to the continuous change of the distribution of inputs at each layer [129]. The changing scale and distribution of inputs at each layer implies that the network has to significantly adapt its parameters at each layer and thereby training has to be slow (*i.e.* use of small learning rate) for the loss to keep decreasing during training (*i.e.* to avoid divergence during training). Therefore, batch normalization was introduced to guarantee more regular distributions at all inputs.

This normalization strategy was inspired by general rules of thumb established for efficient training of ConvNets. In particular, for good generalization performance in ConvNets it is common practice to enforce that all training and testing set samples have the same distribution (*i.e.* through normalization). For example, it has been shown that networks converge faster when the input is always whitened [77,91]. Batch normalization builds on this idea by considering that each layer can be considered as a shallow network. Therefore, it would be advantageous to make sure that the inputs keep the same distribution at each layer and this is enforced by learning the distribution of the training data (using mini-batches) and using the statistics of the training set to normalize each input. More generally, it is also important to remember that, from a machine learning perspective, such a normalization scheme can also make features easier to classify. For example, if two different inputs induce two different outputs, they are more easily separable by a classifier if the responses

lie within the same range and it is therefore important to process the data to satisfy this condition.

Similar to divisive normalization, batch normalization also proved to play an important role in ConvNets. In particular, it has been shown that batch normalization not only speeds up training, but it also plays a non-trivial role in generalization where it was able to outperform previous state-of-the-art on image classification (on ImageNet in particular) while removing the need for Dropout regularization [88].

In comparison, batch normalization is somewhat similar to divisive normalization in the sense that they both make the scale of the inputs at each layer similar. However, Divisive Normalization normalizes the values for each input by dividing it by all other inputs at the same location within the same layer. Batch normalization, on the other hand, normalizes each input with respect to statistics of the training set at the same location (or more accurately of the statistics of a mini-batch containing examples from the entire training set). The fact that batch normalization relies on the statistics of a training set may explain the fact that it improves the generalization power of the representation.

One problem with batch normalization is its dependence on the mini-batch size: It might not properly represent the training set at each iteration, if it is chosen to be too small; alternatively, it can have a negative effect of slowing down training, if it is too big (*i.e.* since the network has to see all training samples under the current weights to calculate the mini-batch statistics). Also, batch normalization is not easily applicable to recurrent neural networks since it relies on statistics calculated over a mini-batch of training samples. For this reason, layer normalization has been proposed in [4]. Layer normalization follows the same procedure proposed in batch normalization and the only difference lies in the way normalization statistics are calculated. While batch normalization calculates statistics over a mini-batch, layer normalization calculates statistics for each input separately using all feature maps or hidden units within any one layer. Consequently, in batch normalization each unit is normalized with different statistics relevant to that unit only, whereas layer norm normalizes all units in the same way.

While layer norm was shown to be effective on language related applications

where recurrent networks are usually more suitable, it failed to compete with ConvNets trained with batch normalization for image processing tasks [129]. One possible explanation proposed by the authors is that in ConvNets all units do not make an equal contribution in the activation of a unit at the output; therefore, the underlying assumption that this is the case in layer normalization (*i.e.* using all units to calculate the statistics of the normalization) does not hold for ConvNets.

Discussion

The common thread across the contributions discussed in this subsection is the fact that they all agree on the important role of normalization in improving the representational power of multilayer architectures. Another important point to note is that they all share the same goal of reducing redundancies in the input as well as bringing it to the same scale even while casting the problem under different forms. Indeed, while early proposals of divisive normalization, *e.g.* [102], explicitly cast the problem as a redundancy reduction problem, newer proposals such as batch normalization [129] are also implicitly enforcing this operation through whitening of the data at each layer. Finally, reflecting back on the normalization problem from a biological perspective, it is important to note that biological systems are also efficient in encoding the statistical properties of natural signals in the sense that they represent the world with small codes. Therefore, one might hypothesize that they are also performing similar operations of divisive normalization to reduce redundancies and obtain those efficient codes.

3.4 Pooling

Virtually any ConvNet model, be it biologically inspired, purely learning based or completely hand-crafted, includes a pooling step. The goal of the pooling operation is to bring a level of invariance to changes in position and scale as well as to aggregate responses within and across feature maps. Similar to the three building blocks of ConvNets discussed in the previous sections, pooling is also supported by biological findings as well as more theory driven investigations. The major debate when it

comes to this layer of processing in convolutional networks is on the choice of the pooling function. The two most widely encountered variations are average and max pooling. This section explores the advantages and shortcomings of each and discusses other variations as described in related literature.

3.4.1 Biological perspective

From a biological perspective, pooling is largely motivated by the behavior of the cortical complex cells [18, 67, 74, 109]. In their seminal work, Hubel and Wiesel [74] found that, just like simple cells, complex cells are also tuned to a specific orientation, but as opposed to simple cells, complex cells exhibit a level of position invariance. They suggest that this result is achieved through some sort of pooling in which the responses of simple cells tuned to the same orientation are pooled across space and/or time as illustrated in Figure 3.9.

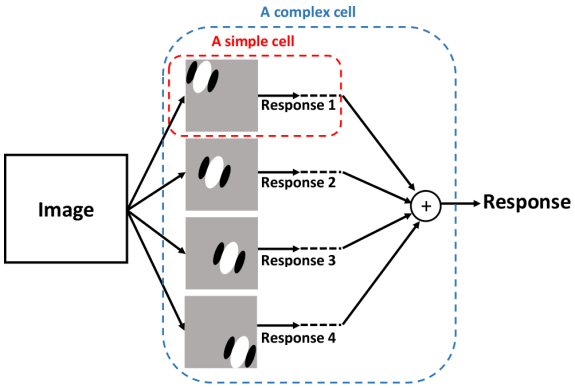

Figure 3.9: An Illustration of the Difference Between Simple and Complex Cells. This illustration suggests that complex cells responses result from combinations of simple cells responses.

Some of the early biologically inspired convolutional networks such as Fukushima's neocognitron [49] and the original LeNet network [91] relied on average pooling. In these efforts, average pooling followed by sub-sampling is largely motivated by the findings of Hubel and Wiesel and it is used to decrease the network's sensitivity to position changes. On the other hand, the HMAX [117] class of networks (*e.g.* [79, 110, 130, 131]) rely on max pooling instead. Supporters of the max pooling strategy claim that it is more plausible when the input to the pooling operator is a set of Gabor filtered images (*i.e.* the typical model for simple cells). In fact, the

authors argue that while a Gaussian scale space (*i.e.* similar to weighted average pooling) reveals new structures at different scales when applied to a natural image, it causes features to fade away when applied to a Gabor filtered image; see Figure 3.10(a). On the other hand, a max pooling operation enhances the strongest responses in the filtered image at different scales as shown in Figure 3.10(b).

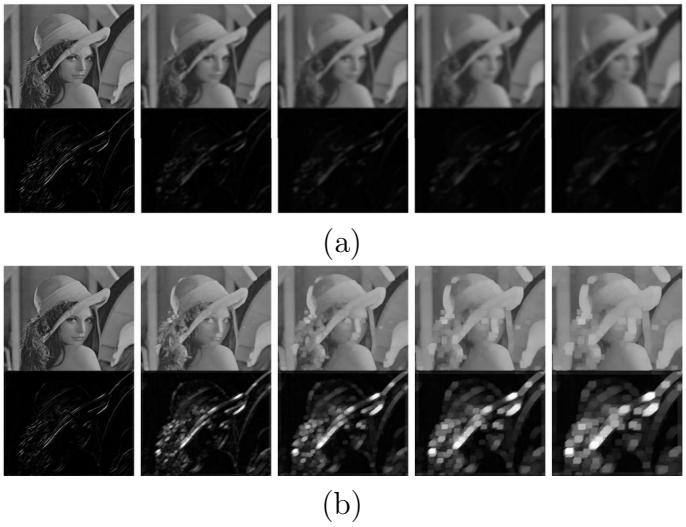

(a)

(b)

Figure 3.10: Average versus Max Pooling on Gabor Filtered Images. This example illustrates the effect of average pooling at various scales when applied to ((a) top row) an original gray-value image and ((a) bottom row) its Gabor filtered version. While average pooling leads to smoother versions of the gray-value image, the sparse Gabor-filtered image fades away. In contrast, the example also illustrates the effect of max pooling at various scales when applied to the same gray-value image ((b) top row) and ((b) bottom row) its Gabor filtered version. Here, max pooling causes the gray-values image to degrade while the sparse edges in the Gabor filtered version are enhanced. Figure reproduced from [131].

The behavior of complex cells can also be viewed as a type of cross-channel pooling, which is in turn another method of injecting invariances into the representation. Cross channel pooling is achieved through the combination of outputs from various filtering operations at a previous layer. This idea was proposed by Mutch and Lowe [110] as an extension to one of the most prominent biologically inspired networks [131], previously introduced in Section 3.1 and illustrated in Figure 3.2. In particular, the authors introduce max pooling across channels at the second layer of their network where the output of the S2 simple cells are pooled across multiple orientations to keep the maximum responding unit at each spatial position as illustrated in Figure 3.11.

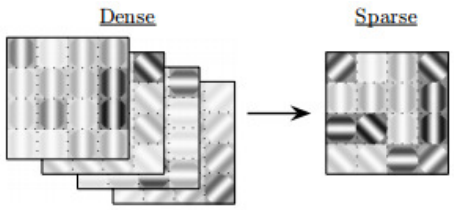

Figure 3.11: Cross-Channel Pooling Illustration. (left) Dense simple cell responses resulting from filtering operations with Gabor filters tuned to various orientations (4 orientations are shown here for illustration purposes) (right) Sparsified simple cell responses resulting from cross-channel pooling using the max operator (*i.e.* for each pixel location, the maximum response across feature maps is kept). Figure reproduced from [110].

Discussion

Overall, based on the description of complex cells, it seems that from a biological perspective both average and max pooling are plausible, although there is more work arguing in favor of average pooling. Independently from the choice of the pooling operator, the fact is that there is general agreement on the existence and significance of pooling. A probably more important question lies in the choice of the receptive field or the units over which pooling is performed. This aspect of the pooling operation is further explored in more theory driven work, as will be described in the next section.

3.4.2 Theoretical perspective

Pooling has been a component of the computer vision representational pipelines for some time, *e.g.* [30, 49, 89, 91, 99], with the goal of introducing some level of invariance to image transformations and better robustness to noise and clutter. From a theoretical perspective, probably one of the most influential works discussing the importance and role of pooling was Koendrink's concept of locally orderless images [87]. This work argued in favor of pooling whereby the exact position of pixels within a Region Of Interest (ROI), *i.e.* a pooling region, can be neglected even while conserving the global image structure. Currently, virtually all convolutional architectures include a pooling block as part of its processing stages. As with biologically motivated models, more theory driven approaches typically employ either average or max pooling.

Recent work approaching their network's design from a purely theory based perspective, *e.g.* ScatNet [15] and SOE-Net [60], rely on a form of average pooling. In particular, their networks rely on a weighted sum pooling operation. These approaches tackle the pooling problem from a frequency domain point of view; therefore, their choice of average pooling is motivated by a desire to keep track of the frequency content of the signal. Average pooling allows these networks to act on different frequencies at each layer while downsampling the images to increase invariance and reduce redundancies. At the same time their controlled approach to specifying pooling parameters allows them to avoid aliasing during the pooling operation. Notably, in SOE-Net's investigation, the superiority of weighted average pooling was empirically demonstrated over both simple box car pooling and max pooling.

Interestingly, most of the early convolutional architectures relied on average pooling as well, *e.g.* [49, 91], but it has slowly fallen out of favor in many learning based convolutional architectures and been replaced by max pooling. This trend has been mainly driven by small differences in performance. However, the role of pooling in a network is significant and needs more careful consideration. In fact, early work exploring the role of pooling [77] demonstrated that the type of pooling plays such a significant role in a ConvNet architecture that even an otherwise randomly initialized network yielded competitive results on the task of object recognition provided the appropriate type of pooling is used. In particular, this work compared average and max pooling and demonstrated that with a randomly initialized network average pooling yields superior performance.

Other work more systematically compared average and max pooling empirically [128] and suggested that there exists a complementarity between the two types of pooling depending on the input type and the transformations it undergoes. Therefore, this work implied that ConvNets can benefit from using more than one pooling option throughout the architecture. Yet other work considered the question from a purely theoretical perspective [12]. Specifically, this work examined the effect of average versus max pooling on the separability of extracted features. The main conclusions of this paper can be summarized in two points. First, the authors argue

that max pooling is more suitable when the pooled features are very sparse (*e.g.* when pooling is preceded by a ReLU). Second, the authors suggest that the pooling cardinality should increase with the input size and that the pooling cardinality affects the pooling function. More generally, it was shown that beyond the pooling type, the pooling size plays an important role as well.

The importance of the pooling cardinality was also explored in various other studies, albeit empirically [27, 81]. Indeed, the role of pooling cardinality was first discussed in the context of the earlier hand-crafted feature extraction pipeline [81]. In particular, this work builds on the spatial pyramid pooling [89] encoding method while highlighting the shortcoming of using predetermined fixed-size pooling grids. The authors suggest learning the pooling windows' sizes as part of the classifier training. More specifically, the authors suggest randomly picking various pooling regions of different cardinalities and training the classifier to pick the pooling region that yields the highest accuracy. The main motivation behind this learning based strategy is to make pooling adaptive to the dataset. For example, the optimal pooling regions for an outdoor scene may lie along the horizon, which does not necessarily apply to indoor scenes. Similarly, for video action recognition it proved more perspicuous to adapt the pooling region to the most salient parts of a video [39]. The role of the pooling window size or cardinality was also directly explored in a neural network context [27]. Here, the authors suggest that features that are most similar should be pooled together. The authors propose finetuning the pooling support (*i.e.* pooling regions) of their network in an unsupervised manner. In particular, pooling windows are chosen to group together similar features according to a pairwise similarity matrix, where the similarity measure is squared correlation. Beyond average and max pooling operations, the common thread across these investigations is the importance of the pooling region independently from the pooling function.

Other work approaches the choice of pooling and its corresponding parameters from a pure machine learning point of view [58, 96, 153]. From this perspective, pooling is advocated as a regularization technique that allows for varying the network's structure during training. In particular, pooling allows for the creation of sub-models within the big architecture thanks to the variation of pathways that a

back propagated signal may take during training. These variations are achieved with methods such as stochastic pooling [153] or cross-channel pooling used in the maxout network [58] and Network in Network (NiN) [96]. NiN was first introduced as a way to deal with overfitting and correct for the over-complete representation of ConvNets [96] . In particular, due to the large number of kernels used at each layer, it was noticed that many networks often end up learning redundant filters after training. Therefore, NiN is introduced to reduce redundancies at each layer by training the network to learn which feature maps to combine using a weighted linear combination. Similar to NiN, the Maxout network [58] introduces cross channel pooling wherein the output is set as the maximum across k feature maps on a channelwise basis. Notably, a recent proposal also relied on cross channel pooling to minimize redundancies [60] even while being completely learning free. In this work, the network is based on a fixed vocabulary of filters and cross channel pooling is designed to group together feature maps resulting from filtering operations with the same kernel. Beyond minimizing redundancies, this approach was adopted to allow the network size to remain manageable, while maintaining interpretability.

Stochastic Pooling (SP) [153] was also introduced as a regularization technique. However, different from maxout and NiN, which perform cross channel pooling, SP acts within a feature map. In particular, stochastic pooling is inspired from the dropout technique that is widely used in fully connected layers, but SP is applied to convolutional layers instead. It relies on introducing stochasticity to the pooling operation that forces the back propagated signal to randomly take different pathways at each iteration during training. The method starts by normalizing feature map responses, a_i, within each region to be pooled, R_j, as

$$p_i = \frac{a_i}{\sum_{k \in R_j} a_k}. \tag{3.11}$$

The normalized values, p_i, are then used as the probabilities of a multinomial distribution, which is in turn used to sample a location l within the region to be pooled. The corresponding activation a_l is the pooled value. Importantly, although stochastic pooling relies on selecting one value from any region R_j (*i.e.* similar to max pooling), the pooled value is not necessarily the largest in R_j. Here, it is important

to note that a different pooling strategy is adopted during testing. At test time, the probabilities are no longer used to sample a location during pooling; instead, they are used as the weights of a weighted sum pooling operation. Hence stochastic pooling is closer in spirit to max pooling during training and closer to average pooling during testing. The authors argue that the adopted pooling strategy during training allows for creating different models thanks to varying pathways, while the pooling used during testing allows for creating a rough average approximation over all possible models seen during training. In summary, stochastic pooling can be seen as an attempt to take the best of both average and max pooling.

Another approach that attempts to achieve a balance between average and max pooling suggests letting the network learn the optimal pooling method [95]. This idea of multiple pooling strategies is motivated by experiments demonstrating that the choice of optimal pooling strategy is affected by the input [128]. In particular, the authors propose three different methods of combining the benefits of average and max pooling, namely; mixed, gated and tree pooling. Mixed pooling combines average and max pooling independently from the region to be pooled, where the network is trained to learn the mixing proportion according to

$$f_{mix}(\mathbf{x}) = a_l f_{max}(\mathbf{x}) + (1 - a_l) f_{avg}(\mathbf{x}), \tag{3.12}$$

subject to the constraint $a_l \in [0, 1]$. In gated max-average pooling the mixing proportion is adaptive to the region to be pooled. In particular, the network is trained to learn a gating mask, $\mathbf{w}$, that is applied to the input data via pointwise multiplication. Using this gating mask, the mixing function is now defined as

$$f_{mix}(\mathbf{x}) = \sigma(\mathbf{w}^T\mathbf{x}) f_{max}(\mathbf{x}) + (1 - \sigma(\mathbf{w}^T\mathbf{x})) f_{avg}(\mathbf{x}), \tag{3.13}$$

with $\sigma(\mathbf{w}^T\mathbf{x}) = \frac{1}{(1+exp(-\mathbf{w}^T\mathbf{x}))}$.

The third pooling strategy proposed in this work is tree pooling, which can be viewed as an extreme version of gated pooling. In tree pooling, not only the mixing proportions are learned but the pooling functions to be combined are learned as well. Specifically, a tree structure is adopted to learn the parameters of the

individual functions and their mixing strategy as well. The difference between the three pooling methods is illustrated in Figure 3.12. In sum, the main idea behind these proposals is letting the pooling strategy adapt to the region being pooled. Following this strategy, the authors were able to demonstrate the value of not only combining average and max pooling but also that of adapting the pooling function to the region to be pooled.

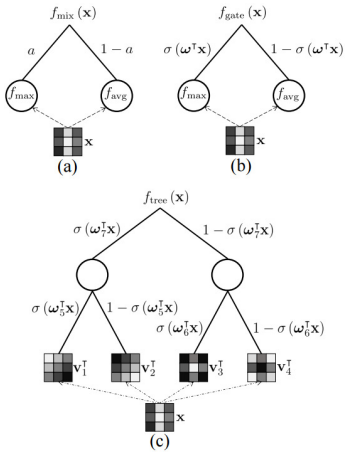

Figure 3.12: Mixed, Gated and Tree Pooling. Illustration of the described (a) mixed max-average pooling, (b) gated max-average pooling and (c) tree pooling. Figure reproduced from [95].

Finally, it is worth mentioning under this section one last type of pooling, referred to as global pooling. Global pooling has been used in some prominent ConvNet models in an effort to deal with more practical issues relevant to ConvNet architecture design [62, 96]. For example, it is known that standard ConvNets rely on convolutional layers for feature learning/extraction and fully connected layers followed by a softmax for classification. However, fully connected layers entail the use of a large number of parameters and are thereby prone to overfitting. Many methods were introduced to deal with overfitting induced by fully connected layers, perhaps the most widely used of which is dropout [88]. However, a more elegant way that fits naturally in a convolutional framework was introduced in NiN [96] and it is called global average pooling. It simply relies on aggregating the last layer features across the entire feature map support. Another example of reliance on global pooling is also found in the so called SPP-Net [62]. In this work, Spatial Pyramid Pooling (SPP) [89], is used to enable convolutional networks to accept input images of any

size. In fact, ConvNets require fixed size input due to the use of fully connected layers. SPP-Net introduces spatial pyramid pooling after the last convolutional layer to correct for this difficulty. In particular, spatial pyramid pooling is used to generate a fixed size representation independently from the size of the input image as illustrated in Figure 3.13. Notably, global average pooling used in NiN, is akin to performing spatial pyramid pooling at the last layer of the ConvNet where the pyramid consists of only the coarsest level.

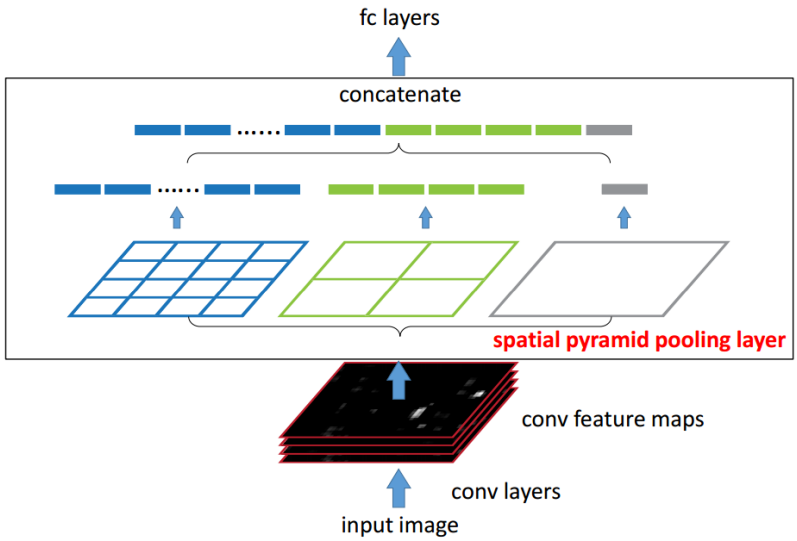

Figure 3.13: Spatial Pyramid Pooling Network. SPP is applied to the feature maps of the last convolutional layer of a network. Because the spatial bins are proportional to the image size, SPP generates feature vectors of the same size independently of the input image size. Hence SPP-Net does not require input images to be pre-processed such that they are of the same size. Figure reproduced from [62].

Discussion

Traditionally, the default functions used in pooling have relied on either the average or max operators. However, several investigations revealed a certain complementary between the two showing that more parameters should be taken into account when choosing the pooling operation. Due to such observations, recent research has been pushing to extend the idea of training to include learning the pooling functions and their parameters. However, this direction entails an increase in the number of parameters to be learned and thereby more chances of overfitting. Importantly, this approach is to be taken with caution as it would likely further obscure our knowl-

edge and understanding of the learned representations. In complement, pooling parameters can be specified on a theoretical basis for cases where previous stages of processing have adequate analytic detail. Overall, pooling should be viewed as a way to summarize information from multiple features into a compact form that preserves the important aspects of the signal while discarding details. Beyond deciding how to summarize the features, it is clear that the harder problem is to determine what constitutes data that should be pooled and where that data is present.

3.5 Overall discussion

This chapter discussed the role and importance of the most widely used building blocks in a typical ConvNet architecture in an effort to understand the working principles of ConvNets. In particular, the details of each block were addressed from both biological and theoretical perspectives. Overall, various common threads emerge from the exploration of the discussed building blocks. In particular, it appears that all blocks find relatively strong motivations from the operations taking place in the visual cortex. Further, although all blocks play a significant role in ConvNets, it appears that the selection of the convolutional kernels is the most important aspect, as evidenced by the larger body of literature tackling this block. More importantly, it seems that more recent ConvNet architectures discussed throughout this chapter (*e.g.* [15, 28, 60, 75, 148]) are aiming at minimizing the need for heavy training based solutions by incorporating more controlled building blocks at various stages of their networks. These recent approaches are in turn motivated by various efforts that revealed the sub-optimality of the learning based ConvNets (*e.g.* predominant redundancies in some of the widely used learned ConvNets) via layerwise visualization and ablation studies, as will be discussed in the next chapter.

Chapter 4

Current Status

The review of the role of the various components of ConvNet architectures emphasized the importance of the convolutional block, which is largely responsible for most abstractions captured by the network. In contrast, this component remains the least understood block of processing given that it entails the heaviest learning. This chapter reviews the current trends in attempting to understand what is being learned at various ConvNet layers. In light of these trends, various critical open problems that remain will be highlighted.

4.1 Current trends

While various ConvNet models continue to push the state-of-the-art further in several computer vision applications, understanding of how and why these systems work so well is limited. This question has sparked the interest of various researchers and in response several approaches are emerging as ways of understanding ConvNets. In general, these approaches can be divided into three tacks: those that rely on visualizations of the learned filters and the extracted feature maps, those that rely on ablation studies as inspired from biological approaches to understanding the visual cortex and those that rely on minimizing learning by introducing analytic principles into their network's design. Each of these approaches will be briefly reviewed in this section.

4.1.1 Understanding ConvNets via visualization

Although several methods have been proposed in the literature for visualizing the feature maps extracted by ConvNets, in this section we will focus on the two most prominent approaches and discuss their different variations.

The first approach to ConvNet visualization is known as a dataset-centric approach [151] because it relies on probing the network with input from a dataset to find maximally responding units in the network. One of the earliest approaches falling under this category is known as DeConvNet [154], where visualization is achieved in two steps. First, a ConvNet is presented with several images from a dataset and the feature maps responding maximally to this input are recorded. Second, these feature maps are projected back to the image space using the DeConvNet architecture, which consists of blocks that invert the operations of the ConvNet used. In particular, DeConvNet inverts the convolution operations (*i.e.* performs "de-convolution") via use of the transpose of the learned filters in the ConvNet under consideration. Here, it is worth noting that taking the transpose is not guaranteed to invert a convolution operation. For "un-pooling", DeConvNet relies on recording the locations corresponding to max-pooled responses in the ConvNet and uses those locations for "un-pooling" or upsampling the feature maps. These operations are summarized in Figure 4.1.

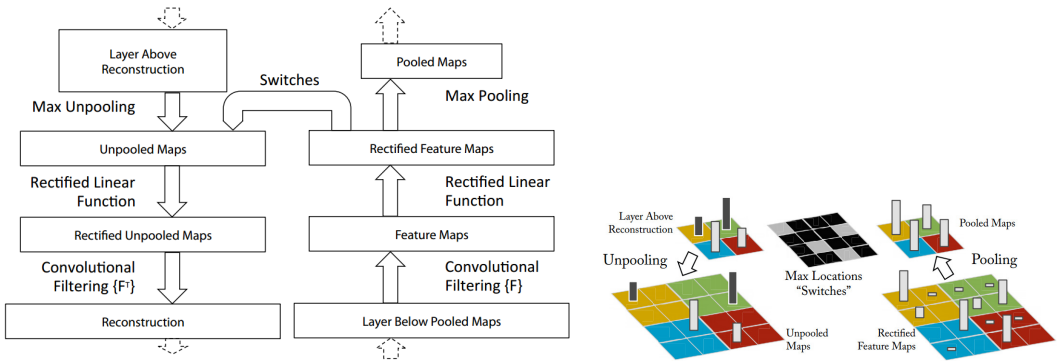

Figure 4.1: DeConvNet building blocks. (a) Illustrates a DeConvNet operation that can be applied to project the feature maps, extracted from any layer of a ConvNet, back to image space. (b) Illustrates the "un-pooling" operation via use of "switches", which correspond to the locations responding to the max pooling operation. Figure reproduced from [154].

Figure 4.2: Visualization obtained by applying DeconvNet at various layer of a standard ConvNet architecture such as AlexNet [88]. Figure reproduced from [154].

Typical visualizations resulting from these methods are shown in Figure 4.2. Overall these visualization reveal that earlier layers in the network tend to capture low level features such as oriented bars and edges, *i.e.* filters learned at lower layers are similar to oriented bandpass filters. In contrast, at higher layers features captured progress from simple textures to more complex objects. Interestingly, these visualizations tend to conserve a high level of detail from the images that yielded a high response in a network. In fact, it seems like these visualization tend to emphasize the edges of the input images and mainly reveal the part of the im-

age that is responsible for the high response (*i.e.* they can be seen as methods for finding the high contrast points of the input images and mainly reveal the part that is responsible for high classification results). Motivated by these observations, other approaches falling under the dataset-centric paradigm proposed even simpler methods to visualize what a network is learning. Examples include methods that progressively remove parts from images yielding high responses to highlight what parts are responsible for high responses [156, 157]. Some of the conclusions that emerged from these approaches are that objects are largely responsible for recognizing scenes [156] or more generally that object detectors emerge as we visualize higher layers of the network [157].

The second approach to ConvNet visualization is known as a network-centric approach [151] because it uses the network parameters only without requiring any additional data for visualization purposes. This approach was first introduced in the context of deep belief networks [37] and later applied to ConvNets [133]. In this case, visualization is achieved by synthesizing an image that will maximize some neuron's (or filter's) response. For example, starting from the last layer of a network that yields a class score, S_c, and an image initialized to random noise, I, the goal is to modify the image such that its score for belonging to class c is maximized. This optimization problem is defined in [133] according to

$$\arg\max_I S_c(I) - \lambda ||I||_2^2, \tag{4.1}$$

where λ is a regularization parameter. Here the L_2 regularization is used to penalize large values. Most other methods falling under this paradigm attempt to solve the same optimization problem while enforcing different regularization techniques such as total variation regularization to enforce smoothness and avoid high frequency content in the synthesized image [104] or simple clipping of pixels that do not participate strongly into the filter's response to only highlight the patterns responsible for a filter's activation [151].

Typical visualization resulting from network-centric approaches when used to maximize class scores as defined in (4.1) are shown in Figure 4.3. Usually, these visualizations suggest that the network is learning high level shapes responsible

for discriminating various objects (*e.g.* eyes, nose and ears when the target class is animals faces); however, the exact locations of these features does not matter. Therefore, these visualizations imply that the network learns invariances progressively (*e.g.* it becomes position agnostic at higher layers), as expected from the use of various pooling operations. However, when this network-centric visualization technique is applied to invert lower layers, it does not necessarily show that they are learning lower level features such as edges as opposed to the dataset-centric technique. For example, in Figure 4.3(b), it is seen that lower layers retain most of the photographic information present in the image. More generally, a major limitation of visualization approaches to understanding ConvNets is the subjective nature of the interpretation, which typically is based on visual inspection by the authors of the method.

4.1.2 Understanding ConvNets via ablation studies

Another popular method to shed light on ConvNet capabilities that is being widely used is the so called ablation study of the network. In fact, many prominent ConvNet papers (*e.g.* [23, 29, 41, 78, 134, 144, 154]) include an ablation study in their experimental section, where the goal is to isolate the different components of the network to see how removing or adding a block affects the overall performance.

These ablation studies have the potential to guide ConvNet practitioner towards "good practices" to achieve higher performance in different applications. For example, one of the earliest ablation studies in the context of ConvNets revealed the importance of proper rectification and normalization even while using randomly initialized networks [77]. Other work, revealed the importance of deeper representations while using smaller filters at all layers [23, 135]. Yet other studies, investigated the role of pre-training and finetuning as well as the number, location and magnitude of features. These investigations, further highlighted the transferability of features extracted from ConvNets across tasks [1].

More interestingly, other work proposed to dissect ConvNets to investigate the effect of each component on the interpretability of the representations learned [6]. This approach relies on a dataset with pixel level annotations, where each pixel is

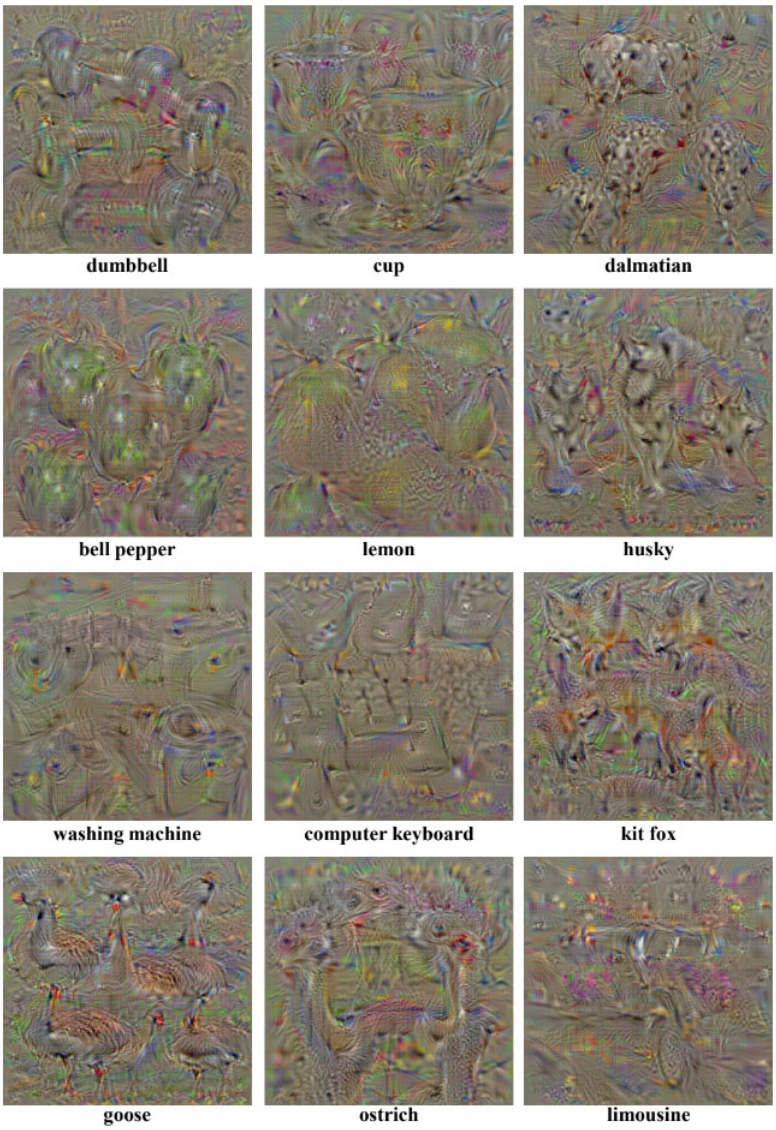

Figure 4.3: Visualization obtained by applying optimization in the image space as done in the network-centric approaches. (a) Visualization obtained by maximizing the score of belonging to various classes, as shown below each image. Figure reproduced from [133]. (b) Visualizations obtained by maximizing the responses of a standard network at various layers, as shown below each image. Figure reproduced from [104].

assigned several "concept" labels that include color, texture, object and scene labels. Each unit in a ConvNet under consideration is evaluated for its ability to generate a segmentation mask that matches a certain concept-based segmentation mask L_c. In particular, each feature map, S_k, in the network is converted to a binary mask, M_k, where pixels are set to 1 only if their activation exceeds a certain pre-set threshold. Next, each unit, k, is assigned a score for its ability to segment a given concept, c, according to

$$IoU_{k,c} = \frac{\sum_{dataset} |M_k \cap L_c|}{\sum_{dataset} |M_k \cup L_c|} \tag{4.2}$$

where $|.|$ is the cardinality of the set. With this measure, the interpretability of each unit is defined based on its ability to generate good segmentation masks. This measure revealed that units in lower layers are able to generate better color or texture based masks, whereas higher layers generate better object and scene segmentations. In line with dataset-centric visualization approaches, this observation suggests that lower layers are learning filters that capture lower level concepts while higher layers learn more abstract features such as objects parts. This approach also allowed for a systematic analysis of the effect of various nonlinearities and training strategies on interpretability and revealed that higher performance does not always yield highly interpretable units. For example, it was shown that regularization techniques such as batch normalization non-trivially affect a unit's interpretability as defined in this approach. Also, it was found that networks trained on scenes datasets yield more interpretable units compared to the widely used ImageNet training. Unfortunately, one of the main flaws of this approach is the fact that their definition of interpretability depends highly on the dataset used for evaluation. In other words, ConvNet units capable of capturing concepts that are not represented in the dataset will yield low IoU scores; hence, deemed not interpretable by this method, even if the concept is visually interpretable. Therefore, this method can miss other important aspects revealed by the network components responsible for higher performance.

4.1.3 Understanding ConvNets via controlled design

Another method to understand ConvNets is to minimize the number of learned parameters by injecting priors into the network design. For example, some methods reduce the number of learned filters per layer and include transformed versions of the learned filters in each layer to model rotation invariances, *e.g.* [100, 158]. Other approaches rely on replacing learned filters with a basis set and instead of learning filter parameters they learn how to combine the basis set to form the effective filters at each layer, *e.g.* [28, 75, 100, 148, 158]. Yet other approaches, push the idea of injecting priors into their network design even further by fully hand crafting their network and adapting it to a given task, which yields especially interpretable networks, *e.g.* [15, 60, 113]. Most of the techniques falling under this paradigm were previously discussed in details in Section 3.1.2 of Chapter 3.

4.2 Open problems

This report documented the significant progress made in the design of various novel ConvNet architectures and building blocks. While this progress resulted in a new state-of-the-art in several computer vision applications, understanding of how these ConvNets achieve those results lags behind. Moreover, there is little understanding of the performance limitations (*e.g.* failure modes) of these approaches. Therefore, shedding light on what information is captured by those ConvNets is becoming particularly relevant. Currently, approaches that focus on understanding ConvNets are becoming apparent in the related literature as discussed throughout this chapter. However, while several of the techniques discussed here are taking good steps, they all leave open critical questions that remain to be answered.

In fact, the review on the different techniques that aim at explaining ConvNets revealed that the most widely adopted approach relies on visualizations. However, one of the biggest flaws of visualization based techniques is the fact that they reduce understanding of a complex and highly nonlinear model to a single image that is open to various potential interpretations. Notably, these visualizations vary according to the adopted technique (*e.g.* dataset-centric versus. network-centric, as shown in Figures 4.2 and 4.3) and usually also depend on the architecture under consideration

as well as the training strategy [6]. Their interpretation also is highly subjective. More importantly, it was shown in a recent study that replacing a strong response of a feature map with random noise and propagating it back through the DeConvNet architecture yields similar visualizations to that obtained when projecting back the feature map response itself [105]. Therefore, this study showed that dataset-centric visualizations do not necessarily reveal what a particular feature map is capturing because they themselves rely on parameters learned by the network to generate their visualizations. Thus, based on this discussion, the following points emerge as potential key ways forward for visualization-based approaches:

- First and foremost, it is of paramount importance to develop ways to make the evaluation of visualizations more objective, via introduction of a metric that evaluates the quality and/or meaning of the generated images.

- Also, while it appears that network-centric visualization approaches are more promising, as they don't rely on a network themselves in generating their visualization (*e.g.* DeConvNet), it appears necessary to standardize their evaluation process as well. One possible solution is to use a benchmark for generating the visualizations and networks trained under the same conditions. Such standardization, can in turn allow for a metric-based evaluation instead of the current interpretation based analysis.

- Another way forward is to visualize multiple units at the same time to better capture distributed aspects of the representations under study, even while following a controlled approach.

Considering ablation studies, while they allow for isolating parts of a network to identify components responsible for better performance, they cannot really elucidate what a network learned as they try to explain ConvNets' highly intertwined components in isolation. Notably, in their current application, ablation studies are simply used as ways to glean a few percentage points in performance without really adding value from an understanding point of view. Here, potentially interesting ways forward for ablation-based approaches include:

- Use of a common and systematically organized dataset that captures different challenges commonly encountered in computer vision (*e.g.* view point and illumination changes) and that entails categories with an increased level of complexity (*e.g.* textures, parts and objects). In fact, an initial dataset of this kind was recently introduced [6]. Use of ablation studies on such a dataset, together with an analysis of the resulting confusion matrices can allow pinpointing the failure modes of ConvNet architectures and thereby lend better understanding.

- In addition, systematic studies of how multiple coordinated ablations impacts performance is interesting. Such studies should extend insight beyond how isolated units perform.

Finally, although there are flaws in both visualization and ablation studies approaches to understanding ConvNets, they still shed some light on ConvNet shortcomings, such as the redundancies in the learned filters (*e.g.* see Figure 3.8) and importance of certain nonlinearities (*e.g.* [23, 77]). These insights were in turn used in more controlled approaches to ConvNet realization that are less reliant on data and more importantly less obscure (*e.g.* [15, 60, 75, 78, 113]). These controlled approaches are emerging as a promising direction for future research as they lend deeper understanding of the operations and representations that these systems employ relative to purely learning based approaches. Indeed, many such insights were reviewed in the previous chapter. In turn, they also have the potential to support more rigorous performance bounds based on their precise system specifications. Here interesting ways forward include:

- Progressively fixing network parameters and analyzing impact on a network's behavior. For example, fixing convolutional kernel parameters (based on some prior knowledge of the task at hand) one layer at a time to analyze the suitability of the adopted kernels at each layer. This progressive approach has the potential to shed light on the role of learning and can also be used as an initialization to minimize training time.

- Similarly, design of the network architecture itself can be investigated (*e.g.*

number of layers or filters per layer) via analysis of the input signal properties (*e.g.* the frequency content of the signal). This method can help adapt the architecture's complexity to the application.

- Finally, use of controlled approaches to network realization can be accompanied with systematic studies of the role of other aspects of ConvNets that usually receive less attention due to the focus on learned parameters. Examples include investigation of various pooling strategies and the role of residual connections when most learned parameters are otherwise fixed.

Bibliography

[1] P. Agrawal, R. Girshick, and J. Malik. Analyzing the performance of multilayer neural networks for object recognition. In *ECCV*, 2014. 4.1.2

[2] S. Amari. Backpropagation and stochastic gradient descent method. *Neurocomputing*, 5(4 - 5):185 – 196, 1993. 2.1.5

[3] M. Andrychowicz, M. Denil, S. Gómez, M. W. Hoffman, D. Pfau, T. Schaul, and N. de Freitas. Learning to learn by gradient descent by gradient descent. In *NIPS*, 2016. 2.1.6

[4] L. J. Ba, R. Kiros, and G. E. Hinton. Layer normalization. *arXiv*, 1607.06450, 2016. 3.3.2

[5] C. L. Baker and I. Mareschal. Processing of second-order stimuli in the visual cortex. *Progress in Brain Research*, 134:171–91, 2001. 3.1.1, 3.1.1, 3.1.2

[6] D. Bau, B. Zhou, A. Khosla, A. Oliva, and A. Torralba. Network dissection: Quantifying interpretability of deep visual representations. In *CVPR*, 2017. 4.1.2, 4.2

[7] Y. Bengio, A. Courville, and P. Vincent. Representation learning: A review and new perspectives. *IEEE Transactions on Pattern Analysis and Machine Intelligence*, 35(8):1798–1828, 2013. 2.1, 2.1.1

[8] Y. Bengio, P. Lamblin, D. Popovici, and H. Larochelle. Greedy layer-wise training of deep networks. In *NIPS*, 2007. 2.1.1

[9] Y. Bengio, P. Simard, and P. Frasconi. Learning long-term dependencies with gradient descent is difficult. *IEEE Transactions on Neural Networks*, 5(2):157–166, 1994. 2.1.2, 2.1.2

[10] U. Bergmann, N. Jetchev, and R. Vollgraf. Learning texture manifolds with the periodic spatial GAN. In *ICML*, 2017. 2.1.4

[11] C. Blakemore and G. Cooper. Development of the brain depends on the visual environment. *Nature*, 228:477–478, 1970. 3.1.1

[12] Y. Boureau, J. Ponce, and Y. LeCun. A theoretical analysis of feature pooling in visual recognition. In *ICML*, 2010. 3.4.2

[13] R. M. Boynton and D. N. Whitten. Visual adaptation in monkey cones: Recordings of late receptor potentials. *Science*, 170(3965):1423–1426, 1970. 3.3.1

[14] G. J. Brouwer and D. J. Heeger. Cross-orientation supression in human visual cortex. *Journal of Neurophysiology*, (106):2108–2119, 2011. 3.3.1, 3.3.1, 3.3.1

[15] J. Bruna and S. Mallat. Invariant scattering convolution networks. *IEEE Transactions on Pattern Analysis and Machine Intelligence*, 35:1872–1886, 2013. 3.1.2, 3.5, 3.1.2, 3.1.2.1, 3.2.2, 3.2.2, 3.4.2, 3.5, 4.1.3, 4.2

[16] A. E. Bryson, W. F Denham, and S. E. Dreyfus. Optimal programming problems with inequality constraints. *AIAA*, 11:2544–2550, 1963. 2.1.5

[17] N. Buduma and N. Locascio. *Fundamentals of Deep Learning: Designing Next-Generation Machine Intelligence Algorithms*. O'Reilly Media, 2017. 2, 2.1, 2.2

[18] M. Carandini. What simple and complex cells compute. *The Journal of Physiology*, 577:463–466, 2006. 3.4.1

[19] M. Carandini and D. J. Heeger. Normalization as a canonical neural computation. *Nature reviews. Neuroscience*, 13:51–62, 2011. 3.3.1, 3.3.1

[20] J. Carreira and A. Zisserman. Quo vadis, action recognition? a new model and the kinetics dataset. In *CVPR*, 2017. 2.3.3

[21] T. H. Chan, K. Jia, S. Gao, J. Lu, Z. Zeng, and Y. Ma. PCANet: A simple deep learning baseline for image classification? *Transactions of Image Processing*, 24:5017–5032, 2015. 3.1.2, 3.1.2.1

[22] K. Chatfield, V. Lempitsky, A. Vedaldi, and A. Zisserman. The devil is in the details: an evaluation of recent feature encoding methods. In *BMVC*, 2011. 2.2.1

[23] K. Chatfield, K. Simonyan, A. Vedaldi, and A. Zisserman. Return of the devil in the details: Delving deep into convolutional nets. In *BMVC*, 2014. 1.1, 2.2.1, 4.1.2, 4.2

[24] L. C. Chen, G. Papandreou, I. Kokkinos, K. Murphy, and A. L. Yuille. DeepLab: Semantic Image Segmentation with Deep Convolutional Nets, Atrous Convolution, and Fully Connected CRFs. *arXiv*, 1606.00915, 2017. 2.2.3

[25] M. Cimpoi, S. Maji, I. Kokkinos, S. Mohamed, , and A. Vedaldi. Describing textures in the wild. In *CVPR*, 2014. 2.1.6

[26] D-A. Clevert, T. Unterthiner, and S. Hochreiter. Fast and accurate deep network learning by exponential linear units. In *ICLR*, 2016. 3.2.2, 3.2.2

[27] A. Coates and A. Y. Ng. Selecting receptive fields in deep networks. In *NIPS*, 2011. 3.4.2

[28] T. S. Cohen and M. Welling. Steerable CNNs. In *ICLR*, 2017. 3.1.2, 3.1.2, 3.1.2.1, 3.5, 4.1.3

[29] J. Dai, H. Qi, Y. Xiong, Y. Li, G. Zhang, H. Hu, and Y. Wei. Deformable convolutional networks. In *ICCV*, 2017. 2.2.2, 2.13, 4.1.2

[30] N. Dalal and B. Triggs. Histograms of oriented gradients for human detection. In *CVPR*, 2005. 3.4.2

[31] P. Dayan and L. F. Abbott. *Theoretical Neuroscience: Computational and Mathematical Modeling of Neural Systems*. The MIT Press, 2005. 3.2.1

[32] A. Dobbins, S. W. Zucker, and M. S. Cynader. Endstopped neurons in the visual cortex as a substrate for calculating curvature. *Nature*, 329:438–441, 1987. 3.1.1

[33] J. Donahue, L. A. Hendricks, M. Rohrbach, S. Venugopalan, S. Guadarrama, K. Saenko, and T. Darrell. Long-term recurrent convolutional networks for visual recognition and description. *IEEE Transactions on Pattern Analysis and Machine Intelligence*, 39(4):677–691, 2017. 2.4, 2.3, 2.3.1, 2.16, 2.3.1

[34] J. Duchi, E. Hazan, and Y. Singer. Adaptive subgradient methods for online learning and stochastic optimization. *Journal of Machine Learning Research*, 12:2121–2159, 2011. 2.1.5

[35] A. Dundar, J. Jin, and E. Culurciello. Convolutional clustering for unsupervised learning. In *ICLR workshops*, 2016. 3.1.2

[36] D. Eigen and R. Fergus. Predicting depth, surface normals and semantic labels with a common muli-scale convolutional architecture. In *ICCV*, 2015. 1.1

[37] D. Erhan, Y. Bengio, A. Courville, and P. Vincent. Visualizing higher-layer features of a deep network. Technical Report 1341, University of Montreal, 2009. 4.1.1

[38] L. Fei-Fei, R. Fergus, and R. Perona. One-shot learning of object categories. *IEEE Transactions on Pattern Analysis and Machine Intelligence*, 28:594–611, 2006. 2.1.6

[39] C. Feichtenhofer, A. Pinz, and R. P. Wildes. Dynamically encoded actions based on spacetime saliency. In *CVPR*, 2015. 2.4, 3.4.2

[40] C. Feichtenhofer, A. Pinz, and R. P. Wildes. Spatiotemporal residual networks for video action recognition. In *NIPS*, 2016. 2.3.3, 2.3.3

[41] C. Feichtenhofer, A. Pinz, and R. P. Wildes. Spatiotemporal multiplier networks for video action recognition. In *CVPR*, 2017. 2.1.6, 2.3.3, 2.3.3, 4.1.2

[42] C. Feichtenhofer, A. Pinz, and R. P. Wildes. Temporal residual networks for dynamic scene recognition. In *CVPR*, 2017. 2.3.2

[43] C. Feichtenhofer and A. Zisserman. Convolutional two-stream network fusion for video action recognition. In *CVPR*, 2016. 2.3, 2.3.3, 2.3.3

[44] J. Feng and T. Darrell. Learning the structure of deep convolutional networks. In *ICCV*, 2015. 3.1.2.1

[45] S. Fidler, G. Berginc, and A. Leonardis. Hierarchical statistical learning of generic parts of object structure. In *CVPR*, 2006. 3.1.2, 3.1.2.1

[46] S. Fidler, M. Boben, and A. Leonardis. Similarity-based cross-layered hierarchical representation for object categorization. In *CVPR*, 2008. 3.1.2

[47] S. Fidler and A. Leonardis. Towards scalable representations of object categories: Learning a hierarchy of parts. In *CVPR*, 2007. 3.1.2, 3.3

[48] J. Freeman, C. M. Ziemba, D. J. Heeger, E. P. Simoncelli, and A. J. Movshon. A functional and perceptual signature of the second visual area in primates. *Nature Neurosience*, 16:974 – 981, 2013. 3.1.1, 3.1.1

[49] K. Fukushima. Neocognitron: A self-organizing neural network model for a mechanism of pattern recognition. *Biological Cybernetics*, 36:193–202, 1980. 1.1, 2.1.3, 2.6, 3.4.1, 3.4.2

[50] K. Fukushima. A neural network model for the mechanism of selective attention in visual pattern recognition. *Systems and Computers in Japan*, 18(1):102–113, 1987. 2.1.3

[51] K. Fukushima and N. Wake. Handwritten alphanumeric character recognition by the neocognitron. *IEEE Transactions on Neural Networks*, 2(3):355–365, 1991. 2.1.3

[52] R. Girshick. Fast R-CNN. In *ICCV*, 2015. 2.2.3, 2.15

[53] R. Girshick, J. Donahue, T. Darrell, and J. Malik. Rich feature hierarchies for accurate object detection and semantic segmentation. In *CVPR*, 2014. 2.1.6, 2.2.3, 2.15

[54] X. Glorot, A. Bordes, and Y. Bengio. Deep sparse rectifier neural networks. In *AISTATS*, 2011. 3.2.2

[55] M. A. Goodale and A. D. Milner. Separate visual pathways for perception and action. *Trends in Neurosciences*, 15(1):20 – 25, 1992. 2.3.3

[56] I. J Goodfellow, Y. Bengio, and A. Courville. *Deep Learning*. MIT Press, 2016. 2

[57] I. J. Goodfellow, J. Pouget-Abadie, M. Mirza, B. Xu, D. Warde-Farley, S. Ozair, A. Courville, and Y. Bengio. Generative adversarial nets. In *NIPS*. 2014. 2.1.4

[58] I. J. Goodfelow, D. Warde-Farley, M. Mirza, A. Courville, and Y. Bengio. Maxout networks. In *NIPS*, 2013. 3.4.2

[59] T. L. Griffiths and Z. Ghahramani. Infinite latent feature models and the indian buffet process. In *NIPS*, 2005. 3.1.2.1

[60] I. Hadji and R. P. Wildes. A spatiotemporal oriented energy network for dynamic texture recognition. In *ICCV*, 2017. 3.1.2, 3.6, 3.1.2, 3.2.2, 3.2.2, 3.3.2, 3.4.2, 3.5, 4.1.3, 4.2

[61] K. He, G. Gkioxari, P. Dollar, and R. Girshick. Mask R-CNN. In *ICCV*, 2017. 2.2.3, 2.15

[62] K. He, X. Zhang, S. Ren, and J. Sun. Spatial pyramid pooling in deep convolutional networks for visual recognition. In *ECCV*, 2014. 3.4.2, 3.13

[63] K. He, X. Zhang, S. Ren, and J. Sun. Delving deep into rectifiers: Surpassing human-level performance on imagenet classification. In *ICCV*, 2015. 3.2.2, 3.2.2

[64] K. He, X. Zhang, S. Ren, and J. Sun. Deep residual learning for image recognition. In *CVPR*, 2016. 1.1, 2.2.1, 2.10, 2.3.2

[65] D. O. Hebb. *The organization of behavior: A neuropsychological theory*. Wiley, New York, 1949. 3.1.1

[66] D. J. Heeger. Nonlinear model of neural responses in cat visual cortex. In M. Landy and J.A. Movshon, editors, *Computational Models of Visual Processing*, chapter 9, pages 119–134. MIT Press, Cambridge, 1991. 3.2.1, 3.2.2, 3.2.2, 3.3.1, 3.3.1, 3.3.1

[67] D. J. Heeger. Normalization of cell responses in cat striate cortex. *Vis. Neuro.*, 9(2):181–197, 1992. 3.2.1, 3.2.2, 3.3.1, 3.3.1, 3.3.1, 3.4.1

[68] G. E. Hinton, S. Osindero, and Y-W. Teh. A fast learning algorithm for deep belief nets. *Neural Computation*, 18(7):1527–1554, 2006. 2.1.1, 2.1.1

[69] G. E. Hinton and R. R. Salakhutdinov. Reducing the dimensionality of data with neural networks. *Science*, pages 504–507, July 2006. 2.1.1

[70] S. Hochreiter and J. Schmidhuber. Long short-term memory. *Neural Computation*, 9(8):1735–1780, 1997. 2.1.2

[71] T. Hong, N. Kingsbury, and M. D. Furman. Biologically-inspired object recognition system with features from complex wavelets. In *ICIP*, 2011. 3.1.1

[72] G. Huang, Z. Liu, L. Van der Maaten, and K. Q. Weinberger. Densely connected convolutional networks. In *CVPR*, 2017. 2.2.1, 2.11

[73] Y. Huang, K. Huang, L. Wang, D. Tao, T. Tan, and X. Li. Enhanced biologically inspired model. In *CVPR*, 2008. 3.1.1

[74] D. H. Hubel and T. N. Wiesel. Receptive fields, binocular interaction and functional architecture in the cat's visual cortex. *The Journal of Physiology*, 160:106–154, 1962. 2.1.3, 3.1.1, 3.1.1, 3.2.1, 3.3.1, 3.4.1

[75] J. H. Jacobsen, J. V. Gemert, Z. Lou, and A. W.M. Smeulders. Structured receptive fields in CNNs. In *CVPR*, 2016. 3.1.2, 3.4, 3.1.2.1, 3.5, 4.1.3, 4.2

[76] M. Jaderberg, K. Simonyan, A. Zisserman, and K. Kavukcuoglu. Spatial transformer networks. In *NIPS*, 2015. 2.2.2, 2.12

[77] K. Jarrett, K. Kavukcuoglu, M. Ranzato, and Y. LeCun. What is the best multi-stage architecture for object recognition? In *ICCV*, 2009. 1.1, 2.1.3, 3.2.2, 3.2.2, 3.2.2, 3.3.2, 3.3.2, 3.4.2, 4.1.2, 4.2

[78] Y. Jeon and J. Kim. Active convolution: Learning the shape of convolution for image classification. In *CVPR*, 2017. 2.2.2, 4.1.2, 4.2

[79] H. Jhuang, T. Serre, L. Wolf, and T. Poggio. A biologically inspired system for action recognition. In *ICCV*, 2007. 3.1.1, 3.1.1, 3.1.2, 3.1.2.1, 3.4.1

[80] S. Ji, W. Xu, M. Yang, and K. Yu. 3D convolutional neural networks for human action recognition. *IEEE Transactions on Pattern Analysis and Machine Intelligence*, 35:1915–1929, 2013. 2.3.2

[81] Y. Jia, C. Huang, and T. Darrell. Beyond spatial pyramids: Receptive field learning for pooled image features. In *CVPR*, 2012. 3.4.2

[82] X. Jin, C. Xu, J. Feng, Y. Wei, J. Xiong, and S. Yan. Deep learning with S-shaped rectified linear activation units. In *AAAI*, 2016. 3.2.2, 3.2.2

[83] D. A. Kaliukhovich and R. Vogels. Divisive normalization predicts adaptation-induced response changes in macaque inferior temporal cortex. *Journal of Neuroscience*, (36):6116–6128, 2016. 3.3.1

[84] A. Karpathy, G. Toderici, S. Shetty, T. Leung, R. Sukthankar, and L. Fei-Fei. Large-scale video classification with convolutional neural networks. In *CVPR*, 2014. 1.1, 2.3, 2.3.2

[85] K. Kavukcuoglu, M. Ranzato, and Y. LeCun. Fast inference in sparse coding algorithms with applications to object recognition. Technical Report CBLL-TR-2008-12-01, Computational and Biological Learning Lab, Courant Institute, NYU, 2008. 2.1.5

[86] D. P. Kingma and J. L. Ba. Adam: A method for stochastic optimization. In *ICLR*, 2015. 2.1.5

[87] J. Koenderink and A. J. Van Doorn. The structure of locally orderless images. *International Journal of Computer Vision*, 31:159–168, 1999. 3.4.2

[88] A. Krizhevsky, I. Sutskever, and G. E. Hinton. Imagenet classification with deep convolutional neural networks. In *NIPS*, 2012. 1.1, 2.1.3, 2.2.1, 2.8, 3.2.2, 3.3.2, 3.3.2, 3.4.2, 4.2

[89] S. Lazebnik, C. Schmid, and J. Ponce. Beyond bags of features: Spatial pyramid matching for recognizing natural scene categories. In *CVPR*, 2006. 3.4.2, 3.4.2

[90] Y. LeCun, Y. Bengio, and G. E. Hinton. Deep learning. *Nature*, 521(7553):436–444, 2015. 2, 2.1

[91] Y. LeCun, L. Bottou, Y. Bengio, and P. Haffner. Gradient-based learning applied to document recognition. *Proceedings of IEEE*, 86:2278–2324, 1998. 1.1, 2.1.3, 2.2.1, 3.1.2, 3.2.2, 3.2.2, 3.3.2, 3.3.2, 3.4.1, 3.4.2

[92] Y. LeCun, J. S. Denker, and S. A. Solla. Optimal brain damage. In *NIPS*, 1990. 3.1.2.1

[93] Y. LeCun, K. Kavukcuoglu, and C. Farabet. Convolutional networks and applications in vision. In *ISCAS*, 2010. 2.5, 2.1.3

[94] C. Ledig, L. Theis, F. Huszar, J. Caballero, A. Aitken, A. Tejani, J. Totz, Z. Wang, and W. Shi. Photo-realistic single image super-resolution using a generative adversarial network. In *CVPR*, 2017. 2.1.4

[95] C-Y. Lee, P. Gallagher, and Z. Tu. Generalizing pooling functions in convolutional neural networks: Mixed, gated, and tree. In *AISTATS*, 2016. 3.4.2, 3.12

[96] M. Lin, Q. Chen, and S. Yan. Network in network. In *ICLR*, 2014. 2.1.6, 2.2.1, 3.4.2, 3.4.2

[97] F. Liu, C. Shen, and G. Lin. Deep convolutional neural fields for depth estimation fom a single image. In *CVPR*, 2015. 1.1

[98] J. Long, E. Shelhamer, and T. Darrell. Fully convolutional networks for semantic segmentation. In *CVPR*, 2015. 2.2.3, 2.14

[99] D. G. Lowe. Distinctive image features from scale-invariant keypoints. *International Journal of Computer Vision*, 60(2):91–110, 2004. 2.4, 3.4.2

[100] S. Luan, b. Zhang, C. Chen, X. Cao, J. Han, and J. Liu. Gabor convolutional networks. *arXiv*, 1705.01450, 2017. 3.1.2, 4.1.3

[101] S. Lyu. Divisive normalization: justification and effectiveness as efficient coding transform. In *NIPS*, 2010. 3.3.2

[102] S. Lyu and E. P. Simoncelli. Nonlinear image representation using divisive normalization. In *CVPR*, 2008. 3.3.2, 3.3.2

[103] A. L. Maas, A. Y. Hannun, and A. Y. Ng. Rectifier nonlinearities improve neural network acoustic models. In *ICML*, 2013. 3.2.2, 3.2.2, 3.2.2

[104] A. Mahendran and A. Vedaldi. Understanding deep image representations by inverting them. In *CVPR*, 2015. 1.1, 4.1.1, 4.3

[105] A. Mahendran and A. Vedaldi. Salient deconvolutional networks. In *ECCV*, 2016. 4.2

[106] M. Minsky and S. Papert. *Perceptrons: An Introduction to Computational Geometry*. MIT Press, Cambridge, MA, USA, 1969. 2.1.1

[107] P. Mishra and B. K. Jenkins. Hierarchical model for object recognition based on natural-stimuli adapted filters. In *ICASSP*, 2010. 3.1.1

[108] A. J. Movshon and E. P. Simoncelli. Representation of naturalistic image structure in the primate visual cortex. *Cold Spring Harbor Symposia on Quantitative Biology*, 79:115 – 122, 2014. 3.1.1

[109] A. J. Movshon, I. D. Thompson, and D. J. Tolhurst. Understanding locally competitive networks. *The Journal of Physiology*, 283:53 – 77, 1978. 3.2.1, 3.4.1

[110] J. Mutch and D. G. Lowe. Multiclass object recognition with sparse, localized features. In *CVPR*, 2006. 3.1.1, 3.4.1, 3.4.1, 3.11

[111] V. Nair and G. E. Hinton. Rectified linear units improve restricted boltzmann machines. In *ICML*, 2010. 3.2.2

[112] J. Y-H. Ng, M. J. Hausknecht, S. Vijayanarasimhan, O. Vinyals, R. Monga, and G. Toderici. Beyond short snippets: Deep networks for video classification. In *CVPR*, 2015. 2.3, 2.3.1

[113] E. Oyallon and S. Mallat. Deep roto-translation scattering for object classification. In *CVPR*, 2015. 3.1.2, 3.1.2.1, 4.1.3, 4.2

[114] A. Radford, L. Metz, and S. Chintala. Unsupervised representation learning with deep convolutional generative adversarial networks. In *ICLR*, 2016. 2.1.4

[115] S. Reed, Z. Akata, X. Yan, L. Logeswaran, B. Schiele, and H. Lee. Generative adversarial text to image synthesis. In *ICML*, 2016. 2.1.4

[116] S. Ren, K. He, R. Girshick, and J. Sun. Faster R-CNN: Towards real-time object detection with region proposal networks. In *NIPS*, 2015. 2.2.3, 2.15

[117] M. Riesenhuber and T. Poggio. Hierarchical models of object recognition in cortex. *Nature Neuroscience*, 2:1019–1025, 1999. 3.1.1, 3.1, 3.2, 3.1.2, 3.4.1

[118] S. Rifai, P. Vincent, X. Muller, X. Glorot, and Y. Bengio. Contractive auto-encoders: Explicit invariance during feature extraction. In *ICML*, 2011. 2.1.1

[119] A. Rodriguez-Sanchez, M. Fallah, and A. Leonardis. Hierarchical object representation in the visual cortex and computer vision. *Frontiers in Comp. Neuro.*, 9:142, 2015. 2.4

[120] A. J. Rodriguez-Sanchez and J. K. Tsotsos. The importance of intermediate representations for the modeling of 2D shape detection: Endstopping and curvature tuned computations. In *CVPR*, 2011. 3.1.1

[121] A. J. Rodriguez-Sanchez and J. K. Tsotsos. The roles of endstopped and curvature tuned computations in a hierarchical representation of 2D shape. *PLOS ONE*, 7(8):1–13, 08 2012. 3.1.1

[122] F. Rosenblatt. The perceptron–a perceiving and recognizing automaton. Technical Report 85-460-1, Cornell Aeronautical Laboratory, 1957. 2.1.1

[123] F. Rosenblatt. *Principles of Neurodynamics*. Spartan Books, Washington, DC, USA, 1962. 2.1.1

[124] S. Ruder. An overview of gradient descent optimization algorithms. *arXiv*, 1609.04747, 2016. 2.1.5

[125] D. E. Rumelhart, G .E. Hinton, and R. J. Williams. Learning representations by back-propagating errors. *Nature*, 323:533–536, 1986. 2.1.1, 2.1.5

[126] O. Russakovsky, J. Deng, H. Su, J. Krause, S. Satheesh, S. Ma, Z. Huang, A. Karpathy, A. Khosla, M. Bernstein, A. C. Berg, and L. Fei-Fei. Imagenet large scale visual recognition challenge. *International Journal of Computer Vision*, 115(3):211–252, 2015. 2.1.3, 2.2.2

[127] A. Santoro, S. Bartunov, M. Botvinick, D. Wierstra, and T. Lillicarp. Meta-learning with memory augmented neural networks. In *ICML*, 2016. 2.1.6

[128] D. Scherer, A. Müller, and S. Behnke. Evaluation of pooling operations in convolutional architectures for object recognition. In *ICANN*, 2010. 3.4.2, 3.4.2

[129] I. Sergey and C. Szegedy. Batch normalization: Accelerating deep network training by reducing internal covariate shift. In *ICML*, 2015. 3.3.2, 3.3.2, 3.3.2

[130] T. Serre, M. Kouh, C. Cadieu, U. Knoblich, G. Kreiman, and T. Poggio. A Theory of Object Recognition: Computations and Circuits in the Feedforward

Path of the Ventral Stream in Primate Visual Cortex. Technical report, 2005. 3.1.1, 3.1.1, 3.4.1

[131] T. Serre, L. Wolf, S. Bileschi, M. Riesenhuber, and T. Poggio. Robust object recognition with cortex-like mechanisms. *IEEE Transactions on Pattern Analysis and Machine Intelligence*, 29:411–426, 2007. 3.1.1, 3.1.1, 3.2, 3.1.2, 3.1.2.1, 3.4.1, 3.10, 3.4.1

[132] W. Shang, K. Sohn, D. Almeida, and H. Lee. Understanding and improving convolutional neural networks via concatenated rectified linear units. In *ICML*, 2016. 3.2.2, 3.8, 3.2.2

[133] K. Simonyan, A. Vedaldi, and A. Zisserman. Deep inside convolutional networks: Visualising image classification models and saliency maps. In *ICLR*, 2014. 1.1, 4.1.1, 4.3

[134] K. Simonyan and A. Zisserman. Two-stream convolutional networks for action recognition in videos. In *NIPS*, 2014. 2.1.6, 2.3, 2.3.3, 2.17, 4.1.2

[135] K. Simonyan and A. Zisserman. Very deep convolutional networks for large-scale image recognition. In *ICLR*, 2015. 2.2.1, 4.1.2

[136] N. Srivastava, G. E. Hinton, A. Krizhevsky, I. Sutskever, and R. Salakhutdinov. Dropout: A simple way to prevent neural networks from overfitting. *Journal of Machine Learning Research*, 15(1):1929–1958, 2014. 2.2.1

[137] R. S. Sutton. Two problems with backpropagation and other steepest-descent learning procedures for networks. In *Conference of the Cognitive Science Society*, 1986. 2.1.5

[138] C. Szegedy, W. Liu, Y. Jia, P. Sermanet, S. Reed, D. Anguelov, D. Erhan, V. Vanhoucke, and A. Rabinovich. Going deeper with convolutions. In *CVPR*, 2015. 2.2.1, 2.9

[139] D. Tran, L. Bourdev, R. Fergus, L. Torresani, and M. Paluri. Learning spatiotemporal features with 3D convolutional networks. In *ICCV*, 2015. 1.1, 2.3, 2.3.2

[140] J. R. Uijlings, K. E. Sande, T. Gevers, and A. W. Smeulders. Selective search for object recognition. *International Journal of Computer Vision*, 104(2):154–171, 2013. 2.2.3

[141] P. Vincent, H. Larochelle, Y. Bengio, and P-A. Manzagol. Extracting and composing robust features with denoising autoencoders. In *ICML*, 2008. 2.1.1

[142] P. Vincent, H. Larochelle, I. Lajoie, Y. Bengio, and P-A. Manzagol. Stacked denoising autoencoders: Learning useful representations in a deep network with a local denoising criterion. *Journal of Machine Learning Research*, 11:3371–3408, 2010. 2.1.1

[143] L. Wang, Y. Qiao, and X. Tang. Action recognition with trajectory-pooled deep-convolutional descriptors. In *CVPR*, 2015. 2.3.3

[144] L. Wang, Y. Xiong, Z. Wang, Y. Qiao, D. Lin, X. Tang, and L. Van Gool. Temporal segment networks: Towards good practices for very deep two-stream convnets. In *ECCV*, 2016. 2.1.6, 2.3.3, 2.3.3, 4.1.2

[145] H. Wei and Z. Dong. V4 neural network model for visual saliency and discriminative local representation of shapes. In *IJCNN*, 2014. 3.1.1

[146] P. Werbos. *Beyond Regression: New Tools for Prediction and Analysis in the Behavioral Sciences*. PhD thesis, Harvard University, 1974. 2.1.5

[147] K. Woodbeck, G. Roth, and H. Chen. Visual cortex on the GPU: Biologically inspired classifier and feature descriptor for rapid recognition. In *CVPR workshops*, 2008. 3.1.1

[148] D. E. Worrall, S. J. Garbin, D. Turmukhambetov, and G. J. Brostow. Harmonic networks: Deep translation and rotation equivariance. In *CVPR*, 2017. 3.1.2, 3.5, 4.1.3

[149] R. A. Yeh, C. Chen, T. Y. Lim, A. G. Schwing, M. Hasegawa-Johnson, and M. N. Do. Semantic image inpainting with deep generative models. In *CVPR*, 2017. 2.1.4

[150] J. Yosinski, J. Clune, Y. Bengio, and H. Lipson. How transferable are features in deep neural networks? In *NIPS*, 2014. 2.1.6

[151] J. Yosinski, J. Clune, A. Nguyen, T. Fuchs, and H. Lipson. Understanding neural networks through deep visualization. In *ICML workshops*, 2015. 4.1.1, 4.1.1, 4.1.1

[152] M. D. Zeiler. Adadelta: An adaptive learning rate method. *arXiv*, 1212.5701, 2012. 2.1.5

[153] M. D. Zeiler and R. Fergus. Stochastic pooling for regularization of deep convolutional neural networks. In *ICLR*, 2013. 3.4.2

[154] M. D. Zeiler and R. Fergus. Visualizing and understanding convolutional networks. In *ECCV*, 2014. 1.1, 2.1.6, 2.2.1, 4.1.1, 4.1, 4.2, 4.1.2

[155] J. Zhang, Y. Barhomi, and T. Serre. A new biologically inspired color image descriptor. In *ECCV*, 2012. 3.1.1

[156] B. Zhou, A. Khosla, À. Lapedriza, A. Oliva, and A. Torralba. Object detectors emerge in deep scene cnns. In *ICLR*, 2014. 4.1.1

[157] B. Zhou, A. Khosla, A. Lapedriza, A. Oliva, and A. Torralba. Learning Deep Features for Discriminative Localization. In *CVPR*, 2016. 4.1.1

[158] Y. Zhou, Q. Ye, Q. Qiu, and J. Jiao. Oriented response networks. In *CVPR*, 2017. 3.1.2, 4.1.3

[159] C. Zzegedy, A. Toshev, and D. Erhan. Deep neural networks for object detection. In *NIPS*, 2013. 1.1